

UNIVERZA V LJUBLJANI
FAKULTETA ZA FARMACIJO

URŠKA ČOTAR

MAGISTRSKA NALOGA

ENOVITI MAGISTRSKI ŠTUDIJSKI PROGRAM FARMACIJA

Ljubljana, 2016

UNIVERZA V LJUBLJANI
FAKULTETA ZA FARMACIJO



URŠKA ČOTAR

**IDENTIFIKACIJA IN ANTIMIKOTIČNA AKTIVNOST
ZAVIRALCEV GLIVNE PROTONSKE ČRPALKE, IZOLIRANIH IZ
LISTOV IN LUBJA DREVESA *LOPHIRA LANCEOLATA* TIEGH. EX
KEY**

**IDENTIFICATION AND ANTIMYCOTIC ACTIVITY OF FUNGAL
PROTON PUMP INHIBITORS ISOLATED FROM THE LEAVES
AND STEM BARK OF *LOPHIRA LANCEOLATA* TIEGH. EX KEY**

UNIFORM MASTER'S STUDY PROGRAMME PHARMACY

Ljubljana, 2016

The master thesis was written based on the research work done from October 2014 to January 2015 at the Department of Drug Design and Pharmacology, Faculty of Health and Medical Sciences, University of Copenhagen, Denmark under co-mentorship of prof. Dan Staerk, PhD and mentorship of assist. prof. Bojan Doljak, PhD. Fungal growth inhibition assays, preparation and activity determination of plasma membrane H⁺-ATPase along with the determination of IC₅₀ were performed in cooperation with PCOVERY, Copenhagen, Denmark.

ACKNOWLEDGEMENTS

I would like to thank my supervisor Bojan Doljak, who accepted the mentorship of this master thesis with great enthusiasm and who supported and guided me during the writing part.

Furthermore, I would like to express my sincere gratitude to prof. Dan Staerk for giving me the opportunity to work in Natural Products Research group at University of Copenhagen and my working mentor Kenneth Thermann Kongstad for his help and guidance during my practical work. I thank all the members of NPR group who warmly accepted me and who were always willing to share their knowledge and experience. I would also like to acknowledge Anne-Marie Lund Winther from for her valuable explanations and comments. Finally, I thank my family and my friends for the best support I could imagine throughout the whole period of my studies.

STATEMENT

I hereby declare that this Master thesis was done by me under supervision of assist. prof. Bojan Doljak, PhD and co-supervision of prof. Dan Staerk, PhD.

Urška Čotar

TABLE OF CONTENTS

ABSTRACT	v
EXTENDED ABSTRACT IN SLOVENE	vi
LIST OF ABBREVIATIONS AND SYMBOLS	ix
1 INTRODUCTION.....	1
1.1 Overview of fungi related problems	1
1.2 Human fungal infections.....	2
1.2.1 Superficial fungal infections.....	2
1.2.2 Subcutaneous fungal infections	2
1.2.3 Systemic mycosis	3
1.3 Antifungal agents, targets, major issues and challenges.....	3
1.4 Plasma membrane H ⁺ -ATPase enzyme as an antifungal drug target	5
1.5 Natural products.....	6
1.5.1 Natural products in drug discovery	6
1.5.2 Natural products as antifungals	6
1.5.3 Natural products research limits.....	7
1.6 HR-BIOASSAY/HPLC-HRMS-SPE-NMR.....	7
1.7 <i>Lophira lanceolata</i> Tiegh. ex Keay	9
1.7.1 Taxonomy.....	9
1.7.2 Description	9
1.7.3 Habitat and geographic distribution	10
1.7.4 Uses	10
1.7.5 Compounds isolated from leaves and stem bark	11
1.7.6 Antifungal activity.....	13
2 AIM AND PLAN	14
3 MATERIALS AND METHODS	16
3.1 Materials	16
3.1.1 Chemicals	16
3.1.2 Plant material.....	16
3.1.3 Fungal cultures	16
3.2 Methods	17
3.2.1 Preparation of the Plasma Membrane H ⁺ -ATPase for Inhibition Assays	17
3.2.2 Determination of Plasma Membrane H ⁺ -ATPase Activity	17
3.2.3 <i>Candida albicans</i> and <i>Saccharomyces cerevisiae</i> Growth Inhibition Assay	18

3.2.4	Extractions	18
3.2.5	Crude extract screening for PM H ⁺ -ATPase inhibition.....	19
3.2.6	High-Resolution PM H ⁺ -ATPase Inhibition Assay and Growth Inhibition Assay	20
3.2.7	HPLC-HRMS-SPE-NMR.....	20
3.2.8	Preparative scale isolation of selected metabolites.....	21
3.2.9	NMR Experiments.....	21
3.2.10	Determination of IC ₅₀ values for PM H ⁺ -ATPase, IC ₅₀ values for Na ⁺ /K ⁺ -ATPase and MIC for 50 % growth inhibition of <i>S. cerevisiae</i> and <i>C. albicans</i>	22
4	RESULTS AND DISCUSSION	23
4.1	Extractions	23
4.2	Crude extract screening for PM H ⁺ -ATPase inhibition	23
4.3	High-Resolution Inhibition Assays.....	25
4.3.1	PM H ⁺ -ATPase Inhibition Assay	25
4.3.2	<i>C. albicans</i> and <i>S. cerevisiae</i> Growth Inhibition Assay	26
4.3.3	Comment on High-resolution screening.....	28
4.4	HPLC-HRMS-SPE-NMR.....	29
4.5	Preparative scale isolation	30
4.6	NMR experiments.....	31
4.6.1	Structure elucidation.....	36
4.7	Antifungal characterization.....	44
4.7.1	PM H ⁺ -ATPase inhibition and structure-activity relationship	45
4.7.2	Fungal growth inhibition	47
4.7.3	Comment on High-Resolution Inhibition Assays.....	48
4.7.4	Na ⁺ /K ⁺ -ATPase inhibition and antifungal selectivity	48
4.7.5	Flavanones and dihydrochalcones as antifungals.....	48
5	CONCLUSION	50
6	REFERENCES.....	52

LIST OF FIGURES

Figure 1: Mechanism of action of antifungal drugs on the market	4
Figure 2: General workflow for identification of individual bioactive agents from plant extracts using HR-BIOASSAY/HPLC-HRMS-SPE-NMR.....	8
Figure 3: <i>Lophira lanceolata</i> (63)	9
Figure 4: Geographic distribution of <i>Lophira lanceolata</i> (63).....	10
Figure 5: Expected workflow	16
Figure 6: PM H ⁺ -ATPase inhibition profile versus concentration for crude extracts	26
Figure 7: HPLC chromatogram at 254 nm (black) overlaid by plasma membrane H ⁺ -ATPase inhibition profile (red bars) of <i>L. lanceolata</i> leaf extract.....	27
Figure 8: HPLC chromatogram at 254 nm (black) overlaid by plasma membrane H ⁺ -ATPase inhibition profile (red bars) of <i>L. lanceolata</i> stem bark extract.	27
Figure 9: HPLC chromatogram at 254 nm (black) overlaid by <i>Saccharomyces cerevisiae</i> growth inhibition profile (red bars) of <i>L. Lanceolata</i> leaf extract.....	28
Figure 10: HPLC chromatogram at 254 nm (black) overlaid by <i>Saccharomyces cerevisiae</i> growth inhibition profile (red bars) of <i>L. Lanceolata</i> stem bark extract.	28
Figure 11: HPLC chromatogram at 254 nm (black) overlaid by <i>Candida albicans</i> growth inhibition profile (red bars) of <i>L. Lanceolata</i> leaf extract.	29
Figure 12: HPLC chromatogram at 254 nm (black) overlaid by <i>Candida albicans</i> growth inhibition profile (red bars) of <i>L. Lanceolata</i> stem bark extract.	29
Figure 13: HPLC chromatogram at 254 nm for leaf extract, used for HPLC-HRMS-SPE-NMR analysis. Peaks numbered 1-6 correspond to compounds 1-6	31
Figure 14: HPLC chromatogram at 254 nm for stem bark extract, used for HPLC-HRMS-SPE-NMR analysis. Peaks numbered 7-11 correspond to compounds 7-11	31
Figure 15: DQF-COSY spectrum of Lanceoloside A (1)	37
Figure 16: ¹ H NMR spectrum of Lanceolatin A (2) (black) overlaid by ¹ H NMR spectrum of Lanceolatin B (3) (red).....	38
Figure 17: HMBC spectrum of 2'',3''-dihydroochnaflavone	40
Figure 18: NOESY spectrum of ochnaflavone 7''-O-methylether (6).....	41
Figure 19: NOESY spectrum of Lophirone F (10).....	42
Figure 20: HMBC spectrum of Lophirone A (8).....	43
Figure 21: COSY spectrum of (1β,2α)-(2,4-dihydroxybenzoyl)-(3β,4α)-di-(4-hydroxyphenyl)-cyclobutane (9)	44

Figure 22: Orthovanadate	46
--------------------------------	----

LIST OF TABLES

Table I: Taxonomic classification of <i>Lophira Lanceolata</i> (59)	9
Table II: Compounds isolated from the stem bark of <i>Lophira lanceolata</i> (63- 68)	11
Table III: Compounds isolated from the leaves of <i>Lophira lanceolata</i> (69-73)	12
Table IV: Plant material	17
Table V: Fungal cultures used for Growth inhibition assays	17
Table VI: Results for the crude extract screening for PM H ⁺ -ATPase inhibition	25
Table VII: Amounts of isolated compounds using preparative scale isolation	32
Table VIII: Peak number, name, structure, retention time, MS and ¹ H NMR data obtained in the HPLC-HRMS-SPE-NMR mode (methanol- <i>d</i> ₄) and ¹ H NMR data obtained after preparative scale isolation of 4 and 6 (DMSO- <i>d</i> ₆)	33
Table IX: IC ₅₀ values for PM H ⁺ -ATPase and Na ⁺ /K ⁺ -ATPase together with MIC for 50 % inhibition of <i>S. cerevisiae</i> and <i>C. albicans</i>	45
Table X: Compounds previously tested for their ability to inhibit PM H ⁺ -ATPase with their corresponding IC ₅₀ s	46

LIST OF EQUATIONS

Equation 1: Chemical reaction catalyzed by PM H ⁺ -ATPase	5
Equation 2: Calculation of % inhibition of PM H ⁺ -ATPase for crude extract screening and high-resolution PM H ⁺ -ATPase inhibition assay	18
Equation 3: Calculation of % growth inhibition of <i>Candida albicans</i> and <i>Saccharomyces cerevisiae</i> for high-resolution growth inhibition assay	19

ABSTRACT

Invasive fungal infections are associated with high risk of morbidity and mortality in immunocompromised patients whose number is rapidly growing. The emergence of new pathogenic strains not susceptible to existing antifungals rapidly changes clinical needs. One of the approaches to address antifungal resistance is the development of novel antifungal agents focusing on new promising molecular targets.

As part of a large screening campaign of African medicinal plants the antifungal potential of *Lophira lanceolata* Tiegh. ex Keay was investigated with the emphasis on secondary plant metabolites targeting the fungal plasma membrane (PM) H⁺-ATPase. Ethyl acetate extracts of both leaves and stem bark inhibited the fungal proton pump and showed a concentration-dependent activity profile. Both extracts were selected for high-resolution fungal PM H⁺-ATPase inhibition screening which implied that peak **2** from the leaf extract and peak **8** from the stem bark extract were responsible for the pharmacological activity exhibited by the crude extracts. Structural elucidation performed by high-performance liquid chromatography-high resolution mass spectrometry-solid-phase extraction-nuclear magnetic resonance spectrometry (HPLC-HRMS-SPE-NMR) led to identification of lanceoloside A (**1**), lanceolatin A (**2**), lanceolatin B (**3**), ochnaflavone (**4**), 2'',3''-dihydroochnaflavone (**5**), ochnaflavone-7''-O-methyleter (**6**), isombamichalcone (**7**), lophirone A (**8**), (1 β ,2 α)-di-(2,4-dihydroxybenzoyl)-(3 β ,4 α)-di-(4-hydroxyphenyl)-cyclobutane (**9**), lophirone F (**10**) and lophirone C (**11**). For compounds **4-6** and **9** this is the first reported isolation from the plant.

Preparative-scale isolation of active metabolites allowed the determination of the IC₅₀ values for PM H⁺-ATPase and Na⁺/K⁺ ATPase along with the MIC for 50 % inhibition of fungal growth of *S. cerevisiae* and *C. albicans*. Lanceolatin A (**2**) and lophirone A (**8**) are both potent, although poorly selective inhibitors of PM H⁺-ATPase (IC₅₀=13.5 μ M and 15.1 μ M, respectively) but with no effect on fungal growth. For both compounds this is the first time their potential antifungal activity is reported.

The hit compounds, lanceolatin A and lophirone A, represent a starting point for the preparation of more potent semisynthetic analogues with improved permeability and selective toxicity.

Key words: *Lophira lanceolata*, HPLC-HRMS-SPE-NMR, fungal plasma membrane H⁺-ATPase inhibitors, high-resolution enzyme inhibition profiling, antifungal activity.

EXTENDED ABSTRACT IN SLOVENE

RAZŠIRJEN POVZETEK V SLOVENŠČINI

Glivične okužbe vsako leto prizadenejo več kot milijardo ljudi po vsem svetu. Kljub dejstvu, da je večina okužb površinskih, in da se le-te uspešno odzivajo na trenutno dostopne antimikotike, so invazivne glivične okužbe povezane z visoko stopnjo umrljivosti pri imunsko oslabljenih osebah. Ker sta tako glivna kot tudi človeška celica evkarionski, je razvoj antimikotikov z ustrezno selektivno toksičnostjo zelo zahteven. Pojav vedno novih rezistentnih sevov pa hitro spreminja potrebe v praksi. Človek je izpostavljen toksičnim učinkom gliv ter sekundarnih metabolitov plesni, mikotoksinom, tudi preko kontaminirane hrane ter vdihovanja spor iz okolja.

Cilj magistrske naloge je identifikacija in vrednotenje antimikotičnega potenciala spojin iz listov in lubja drevesa *Lophira lanceolata* Tiegh. ex Keay. *Lophira lanceolata* je afriško drevo, ki se uporablja v tradicionalni medicini lokalnega prebivalstva. Rezultati predhodnih študij nakazujejo, da imajo izvlečki listov šibko antimikotično delovanje. Spojinam, ki so že bile izolirane iz listov in lubja in so značilne za rastlino, raziskovalcem še ni uspelo pripisati farmakološkega učinka.

Kot tarčo, preko katere smo ovrednotili protiglivno delovanje izvlečkov in izoliranih spojin, smo izbrali glivno protonsko črpalko plazemske membrane. Gre za obetavno tarčo novih antimikotikov, za katero je bilo dokazano, da je bistvenega pomena za rast glivne celice. PMA1 gen, ki zapisuje za encim, je močno ohranjen med različnimi vrstami gliv in se bistveno razlikuje od genov, ki zapisujejo za primerljive encime sesalcev in rastlin.

V prvem koraku smo etilacetatne izvlečke listov in lubja pripravili v treh koncentracijah in ovrednotili njihovo sposobnost zaviranja glivne H⁺-ATPaze plazemske membrane. Tako izvlečki listov kot tudi izvlečki lubja so uspešno zavrla delovanje encima ter izkazali od koncentracije odvisen profil zaviranja.

Za pripravo profilov visoke ločljivosti smo izvlečka kromatografsko ločili, kar nam je omogočilo pridobitev HPLC profilov z dobro ločbo kromatografskih vrhov pri 254 nm. Eluat posameznega izvlečka smo zbrali v dve mikrotitrski plošči s 96 vdolbinami (retencijski časi 5-35 min listi; retencijski časi 4-34 min lubje), pri čemer smo dobili 88 µL frakcije in ločljivost 5.3 točke/minuto. Vsaki mikrofrakciji smo izmerili *in vitro* sposobnost zaviranja H⁺-ATPaze in zaviranja rasti gliv *C. albicans* in *S. cerevisiae*. Rezultat vsake mikrofrakcije smo izrisali na mesto njenega retencijskega časa in ugotovili, da sta vrh **2** iz izvlečka listov ter vrh **8** iz izvlečka lubja odgovorna za zaviranje H⁺-ATPaze, ki sta ga izvlečka izkazala

prvem delu naše študije. Nobeden izmed vrhov ni pokazal povezave z zaviranjem rasti testiranih gliv. Pri vseh biokromatogramih smo opazili nepravilnosti: negativne meritve absorbance in pozitivne meritve pri časih, kjer se nobena spojina ni eluirala. Poleg tega je pri profilih zaviranja rasti *C. albicans* prišlo do sistemske napake, kar je razvidno iz ponavljanja enakega vzorca izmerjenih aktivnosti v enakih časovnih intervalih skozi celoten časovni okvir testa. Zaradi omenjenih težav smo podvomili v ustreznost in zanesljivost izvedenih testov, vendar je podrobna karakterizacija spojin ob koncu študije potrdila ugotovitve, ki so jih ponudili profili visoke ločljivosti.

Pred poskusom identifikacije spojin s pomočjo sklopljene tehnike HPLC-HRMS-SPE-NMR (tekočinska kromatografija visoke ločljivosti-masna spektrometrija visoke ločljivosti-ekstrakcija na trdni fazi-jedrsko magnetna resonanca), smo metodo za ločbo izvlečka listov optimizirali z namenom boljše ločbe spojin **3** in **4**. Odločili smo se za identifikacijo vseh metabolitov, ki so na podlagi molekulskih mas nakazovali na strukturno podobnost z aktivnima spojinama **2** in **8**. Identifikacija takšnih spojin nam omogoča boljše razumevanje odnosa med strukturo in aktivnostjo zaviralcev glivne protoske črpalke.

Spojinam **1-11** smo posneli masni spekter visoke ločljivosti ter 1D ^1H NMR in 2D NMR (DQF-COSY, NOESY, HSQC, HMBC) spektre. NMR spektri v HPLC-HRMS-SPE-NMR načinu so bili posneti v metanolu- d_4 . ^1H NMR spektra za spojini **4** in **6** sta pokazala nizko razmerje S/N, zato smo obe spojini izolirali in ugotovili, da sta v metanolu- d_4 netopni. Omenjeni dogodek se je izkazal za edino slabost uporabe sklopljene metode za identifikacijo spojin iz kompleksnih mešanic. Vse zgoraj omenjene analize smo zato za spojini **4** in **6** opravili v DMSO- d_6 . Na podlagi posnetih spektrov je bila spojina **1** identificirana kot lanceolose A, **2** kot lanceolatin A, **3** kot lanceolatin B, **4** kot ohnaflavon, **5** kot 2'',3''-dihidroohnaflavon, **6** kot ohnaflavon 7''-O-metil eter, **7** kot izombamihalkon, **8** kot lofiron A, **9** kot 1 β ,2 α -di-(2,4-dihidroksibenzoil)-(3 β ,4 α)-di-4-hidroksifenil-ciklobutan, **10** kot lofiron F in **11** kot lofiron C. Spojine **1-3**, **7**, **8**, **10** in **11** so bile predhodno izolirane iz listov ali lubja drevesa *Lophira lanceolata*, medtem ko so bile spojine **4-6** in **9** prvič izolirane iz omenjene rastline. Biflavonoidi **4-6** so bili predhodno izolirani iz rastlin družine Ochnaceae, v katero spada tudi *Lophira lanceolata*. Spojina **10** je bila samo enkrat prej izolirana in sicer iz korenin *Agapanthus africanus* (Liliaceae).

V zadnjem koraku smo zaviralce glivne protoske črpalke **2** in **8** skupaj s strukturno podobno spojino **3** izolirali ter jim določili IC_{50} za glivno H^+ -ATPazo plazemske membrane in MIC za 50 % zmanjšanje rasti gliv *C. albicans* in *S. cerevisiae*. Izoliranim spojinam smo določili

tudi IC_{50} za Na^+/K^+ -ATPazo, najbolj podobno strukturo glivni protonski črpalki, ki jo najdemo v celici sesalcev. Lanceolatin B (**2**) je bil neaktiven v območju topnosti v DMSO. Lanceolatin A (**2**) in lofiron A (**8**) sta podobno močno zavrla H^+ -ATPazo plazemske membrane (IC_{50} 13.5 μ M in 15.1 μ M). Njihova jakost pa je zelo podobna jakosti spojin, izoliranih iz drugih afriških rastlin. Za večino teh spojin, vključno z aktivnima metabolitoma iz rastline *L. lanceolata*, je značilen flavanonski ali dihidrohalkonski skelet. 2'',3''-dihidroohnaflavon (**5**) se od lanceolatina A (**2**) razlikuje le v mestu povezave med flavanonskim in flavonskim obročem. Medtem ko se ohnaflavon (**4**) razlikuje tudi v prisotnosti dvojne vezi na mestu 2-3 in tako ne vsebuje flavanonskega skeleta. V profilu visoke ločljivosti je **5** izkazal zaviralno aktivnost na glivno H^+ -ATPazo plazemske membrane, **4** pa ne, kar je potrdilo domnevo, da je za učinek odgovoren flavanonski obroč. Lanceolatin A in lofiron A nista zavrla rasti testiranih gliv, *S. cerevisiae* in *C. albicans*, pri koncentracijah nižjih od 150 μ M. Vzrok za to je najverjetneje slaba permeabilnost spojin preko celične stene in/ali celične membrane in aktivnost glivnih iztočnih črpalk. Obe spojini sta izkazali slabo selektivnost za izbrani encim (IC_{50} za Na^+/K^+ ATPazo = $3.0 \pm 0.3 \mu$ M in $40.9 \pm 23.8 \mu$ M).

Obe spojini zaradi svojega zaviralnega delovanja na glivno protonsko črpalko predstavljata dobro izhodišče za pripravo analogov s flavanonskim in dihidrohalkonskim skeletom z izboljšanimi lastnostmi. V nadaljevanju bi bilo treba določiti način vezave spojin v aktivno mesto encima in strukturo le-tega, kar bi omogočilo sintezo analogov s še močnejšim zaviralnim delovanjem. Pri tem bi morali biti pozorni na njihove fizikalno-kemijske lastnosti z namenom izboljšanja permeabilnosti v glivno celico. Koristno bi bilo preučiti vezavo spojin na encime, ki so sorodni glivni protonski črpalki in so prisotni v celicah sesalcev ter tako izboljšati selektivno toksičnost pripravljenih spojin.

Ključne besede: *Lophira lanceolata*, HPLC-HRMS-SPE-NMR, zaviralci glivne H^+ -ATPaze plazemske membrane, profil visoke ločljivosti zaviranja encima, antimikotična aktivnost.

LIST OF ABBREVIATIONS AND SYMBOLS

ΔM	mean error
2D	two-dimensional
ADP	adenosine diphosphate
ATP	adenosine triphosphate
ATPase	adenosine triphosphatase
br	broad signal
c	concentration
DMSO	dimethyl sulfoxide
DMSO- d_6	deuterated dimethyl sulfoxide
DQF-COSY	double quantum filtered correlation spectroscopy
HIV	human immunodeficiency virus
HMBC	heteronuclear multiple-bond correlation spectroscopy
HPLC	high-performance liquid chromatography
HR-BIOASSAY	high-resolution bioassay
HRMS	high-resolution mass spectrometry
HSQC	heteronuclear single-quantum correlation spectroscopy
IC ₅₀	half maximal inhibitory concentration
J	J -coupling
m	multiplicity
MF	molecular formula
MFC	minimal fungicidal concentration
MIC	minimal inhibitory concentration
MOPS	3-(<i>N</i> -morpholino)propanesulfonic acid
MS	mass spectrometry
m/z	mass-to-charge ratio
nH	number of protons
NMR	nuclear magnetic resonance
NOESY	nuclear overhauser effect spectroscopy
OD	optical density
PDA	photodiode array
PM	plasma membrane

RPMI medium	Roswell Park Memorial Institute culture medium
RT	retention time
S/N	signal to noise ratio
SPE	solid-phase extraction
UV	ultraviolet
YPD agar	yeast extract peptone dextrose agar

1 INTRODUCTION

1.1 Overview of fungi related problems

Fungi are taxonomically classified as one of the six kingdoms besides Animalia, Plantae, Chromista, Protozoa and Bacteria (1, 2). The chlorophyll-free eukaryotic kingdom ranges from single celled microscopic yeasts to multicellular filamentous moulds and macroscopic organisms, often referred to as “mushrooms” (3). Despite offering a wide variety of applications in pharmaceutical and food industry, agriculture likewise biotechnology (4-7) some species are capable of colonizing agriculturally significant crops such as rice, wheat, barley, oat, and maize causing severe socio-economic consequences. It has been estimated that 5-10 % of the world’s food production is lost due to fungal spoilage manifested as discoloration, off-flavours, quality decline and nutritional losses (8). Since the cereal trade is increasingly globalized and agricultural crops are spreading outside their original environment and thus exposed to new pathogens against whom they did not have develop efficient defence mechanisms, it is reasonable to expect a rise in fungal infections. However, the biggest issue of crop’s fungal diseases remain mycotoxins, i.e. vertebrate-toxic secondary metabolites produced by moulds colonizing the plant. Mycotoxins can therefore arise in food chain, either by being eaten directly by humans or by being present in animal feed. Some of them are resistant to decomposition, animal digestion, temperature treatments thus remaining in meat and dairy products. Consequently, humans are exposed to their toxic effects (9). It has been predicted that approximately 25 % of the world’s agricultural goods are contaminated with mycotoxins (10). In addition, they can also be introduced into the body by inhalation of airborne spores or through skin. Mycotoxins can be acutely toxic, immunosuppressive, carcinogenic, mutagenic, genotoxic, teratogenic, neurotoxic, hepatotoxic, nephrotoxic, estrogenic (11, 12).

However, the major concern for humans are fungal infections which are still considered to be a global public health problem affecting over a billion of people each year. Recent studies suggest that the fungal infection rate is increasing (13, 14). Most infections are superficial which are rarely dangerous and can be readily and successfully treated with existing antifungal agents and thus having limited impact on the quality of people’s life. Their importance lies in their high incidence and a worldwide distribution (15). On the other hand, invasive fungal infections are associated with high risk of morbidity and mortality in immunodeficient persons. Among groups that are most vulnerable to fungal systemic

infections are patients with hematologic malignancies (leukaemia, lymphomas, myeloma), individuals undergoing hematopoietic stem cell transplantation, organ transplantation (liver, kidney), mayor surgery (e.g. gastrointestinal surgery) or cancer therapy, patients with HIV, diabetes mellitus, renal failure, burns, patients on immunosuppressive therapy (corticosteroids), extended use of antibiotics, prolonged hospitalization, premature babies and people of advanced age. Infections in the above mentioned groups are considered to be opportunistic since the causative agents do not cause diseases in healthy individuals but may be associated with severe disorders in immunocompromised hosts (16). The number of high risk patients is increasing due to major advances in medicine allowing a growing number of organ transplants coupled with the increased use of immunosuppressive drugs likewise an increased survival of critically ill patients. An equally important factor is the HIV disease epidemic. In addition, population aging is itself a risk factor (17).

1.2 Human fungal infections

1.2.1 Superficial fungal infections

Superficial fungal infection are limited to the outermost layers of the skin, scalp and nails. The prevailing cause represent dermatophytes of three genera: *Epidermophyton*, *Trichophyton* and *Microsporum*. By metabolizing keratin dermatophytes cause a variety of clinical conditions, e.g. tinea corporis (infection of body surfaces, especially arms and legs), tinea pedis (infection of the foot), tinea curis (infection of the groin), tinea capitis (infection of scalp hair), and tinea unguium (infection of the nail) (18). Infections caused by species of genus *Candida*, the most frequent being *Candida albicans*, result in medical conditions ranging from local mucocutaneous infections to widespread dissemination with multisystem organ failure. The most common local infections include oropharyngeal candidiasis or thrush, oesophageal candidiasis and vulvovaginal candidiasis. They arise as a result of changes in the normal flora and in patients with weak immune system (19). Pytriasis versicolor caused by yeast in the genus *Malassezia* is a common skin infection with a high incidence in tropical regions. Some mould species also infect skin or nails. Mould mycoses are most likely caused by *Scopulariopsis brevicaulis*, *Scytalidium dimidiatum*, *Fusarium* spp and *Aspergillus* spp (18).

1.2.2 Subcutaneous fungal infections

Subcutaneous fungal infections involve the dermis, subcutaneous tissues, muscles, fascia and even bones. Infections are chronic, difficult to treat although rare. They occur when the causative agent enters the body through skin lesions. The most common infections are mycetoma (caused by *Pseudallescheria*, *Trematosphaeria*, *Acremonium*, *Madurella* etc.), chromoblastomycosis (caused by *Fonsecaea*, *Phialophora*, *Cladophialophora* etc.) and sporotrichosis (caused by *Sporothrix* spp) (18).

1.2.3 Systemic mycosis

Opportunistic fungal infections

Some fungal species are opportunists, i.e. not harmful for immunocompetent hosts but pathogenic for immunocompromised patients whose normal defence mechanisms are impaired (see 1.1). Opportunistic fungal infections include candidiasis (caused by *Candida albicans*), cryptococcosis (caused by *Cryptococcus neoformans*), aspergillosis (caused by *Aspergillus fumigatus*), pseudallescheriasis (caused by *Pseudallescheria boydii*) and zygomycosis or mucormycosis (caused by *Rhizopus*, *Mucor*, *Rhizomucor*, etc.) (18, 20).

Primary fungal infections

Primary fungal infections can affect healthy, immunocompetent individuals. The infection generally starts in the lungs as a result of inhalation of fungal spores. The first manifestation of the disease is usually a localized pneumonia and lung lesions may occur but progress slowly. Systemic mycosis have a chronic course and can spread to several organ systems. Diagnosis of the disease is often late since symptoms are unspecific and include fever, anorexia, night sweats and depression. Primary pathogens are generally dimorphic and geographically restricted. The most common infections are histoplasmosis (caused by *Histoplasma capsulatum* and *Histoplasma dubosii*), coccidioidomycosis (caused by *Coccidioides immitis*) and blastomycosis (caused by *Blastomyces dermatitidis*) (18, 20).

1.3 Antifungal agents, targets, major issues and challenges

The history of medical mycology began in the thirties of the 19th century with the discovery of tinea favosa, but it was not until hundred years later, in 1939, that griseofulvin, the first effective and safe antifungal agent was discovered (21). The development of antifungal agents was considerably slower in comparison to the progress in antibacterial chemotherapeutics which was primarily due to the relatively low incidence of serious fungal

diseases compared to bacterial infection rates but also because fungal and human cells are both eukaryotic thus sharing several similarities in contrast to bacterial prokaryotic cell. Consequently, the achievement of a total selective toxicity i.e. highly toxic to fungi while retaining the host cell intact, was and still is on one of the biggest challenges in the development of antifungals (21, 22). The inability of an agent to obtain a good selectivity leads to adverse events in patients. An example is the nephrotoxicity exhibited by amphotericin B which was long considered the gold standard in management of severe systemic mycosis. However, there are novel lipid formulations available that increase its safety profile but also the costs of treatment. The drugs currently on the market target ergosterol, the principal sterol in fungal membrane (polyenes: amphotericin B, nystatin) and its biosynthesis pathway (azoles: ketoconazole, fluconazole, itraconazole, voriconazole, posaconazole, allylamines: terbinafine, morpholines: amorolofine), cell wall constituents (echinocandins target β 1, 3-glucan: caspofungin, micafungin, anidulafungin), nucleic acid synthesis (flucytosine) and nuclear division (griseofulvin) (Figure 1) (23).

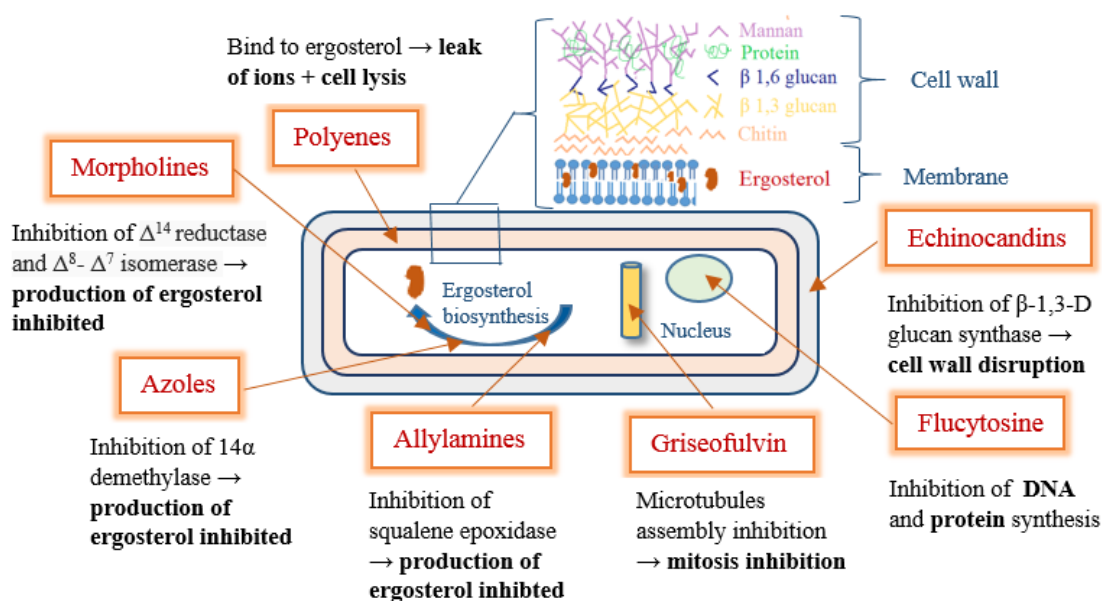


Figure 1: Mechanism of action of antifungal drugs on the market (adapted from 23).

Despite a significant progress in antifungals research in the last fifty years, leading to a successful breakthrough of different classes of agents the main problem remains the rapidly changing needs in clinical practice. Mainly due to the emergence of resistance and cross-resistance repeatedly mentioned in connection to azole class drugs but also because of the

newly emerging pathogen strains which are not susceptible to existing drugs (24). The above mentioned facts suggest a critical need to put effort into the research of novel antifungal drug targets that are widely represented in fungi and hence, having a broad spectrum of susceptible species.

1.4 Plasma membrane H⁺-ATPase enzyme as an antifungal drug target

Plasma membrane (PM) H⁺-ATPase enzyme is an integral membrane protein that belongs to the P-type ATPase family of ion translocating ATPases. It transports protons across the membrane using ATP hydrolysis for energy (see Equation 1) allowing the maintenance of the transmembrane electrochemical proton gradient necessary for nutrient uptake and the regulation of intracellular pH (25).



Equation 1: Chemical reaction catalysed by PM H⁺-ATPase

The PM H⁺-ATPase enzyme consists of 10 transmembrane helices. Over 80 % of the protein is exposed to the cytoplasmic side of the cell, approximately 15 % is estimated to be located in the lipid bilayer while the remaining 5 % is in the extra cytoplasmic phase of the cell (26). It has not only been demonstrated that the PMA1 gene encoding for the enzyme is highly conserved among divergent group of fungi but also that the amino acids of the enzyme significantly differ from comparable structures in the P-type ATPases of mammals and plants (27). Consequently, making it a target that would enable a good selective toxicity and thus limit the potential side effects in patients and at the same time offering a broad-spectrum activity. Furthermore, gene disruption experiments showed that the PM proton pump is one of the few antifungal targets that is essential for growth of a fungal cell (28) and omeprazole-induced inhibition of the enzyme was fungicidal (29). Members of the P-type ATPase class include H⁺/K⁺ ATPase and Na⁺/K⁺ ATPase, targets for several anti-ulcer drugs and cardiac glycosides, respectively. As the drugs that inhibit these enzymes act from the outer side of the membrane, it has also been demonstrated that PM H⁺-ATPase can be inhibited via an interaction with the extracellular surface of the enzyme. Hence, potential antifungal agents targeting the PM proton pump would not be substrates to multidrug resistant pumps as seen in the mechanism of resistance to azoles (30). To sum up, PM H⁺-ATPase is a promising target for new antifungal agents.

1.5 Natural products

Natural products are small molecular-weight organic compounds, secondary metabolites, produced by living organisms; bacteria, fungi, animals and plants. In contrast to primary metabolites they are not indispensable for growth, development nor reproduction. They are biosynthesized mainly by immobile organisms as a response to threats in their environment as a defence mechanism in order to survive and enhance their competitiveness (31, 32).

1.5.1 Natural products in drug discovery

Natural products have always played a major role in traditional medicine due to the common usage of crude therapeutic extracts from plants for a wide range of clinical conditions. Till now they have been the major source of lead compounds for new drugs and thus considered invaluable in the drug discovery process (31). Trends in research and development of new drugs are difficult to define since it takes on average a decade between the discovery of a potential drug candidate to its launch to the market (33). There has been a large decline of interest in natural products during the 90s and the beginning of 2000s (31) primarily due to complexity and variability of the materials, difficult access and challenging development with associated costs and time exposure as well as the fear to “rediscover” compounds that have already been isolated (31, 33). At the same time combinatorial chemistry generated large libraries of synthetic molecules which could have been readily tested via high-throughput screenings and *in silico* methods (31, 34). However, it has been soon noticed that such libraries lack the structural diversity of natural products which have always been a source of inspiration for researchers (34). For this reason, scaffolds of natural products have been introduced as models for combinatorial synthetic libraries and virtual screening methods have also been applied to natural products databases (35, 36).

1.5.2 Natural products as antifungals

The majority of natural products and their derivatives that have been launched to the market so far are indicated for infectious diseases and cancer (37). In fact, three of the major classes of antifungals currently in use are derived from natural products (polyenes, echinocandins and griseofulvin) (38).

Living organisms are exposed to a wide variety of pathogenic fungal strains throughout their life cycle and have been compelled to develop antifungal metabolites to survive (39, 40). It is therefore legitimate to expect that the inhibitors of PM H⁺-ATPase are among plant's

secondary metabolites (27). In addition, it has been suggested that a very limited amount of world's plant biodiversity has been screened for bioactivity so far (41) which means that many compounds are waiting to be discovered and used as novel lead compounds.

1.5.3 Natural products research limits

The major limit of exploring plant extracts as new drug leads is their high complexity, as they contain a large variety of compounds that need to be isolated and purified in order to elucidate the structure of the agent that is responsible for the bioactivity exhibited by the extract (42). With traditional methods it could take several months to come to satisfactory results which is inevitably linked to large financial investments (43, 44). Moreover, the implementation of automated, high-throughput methods appeared to be impossible since the required scale of isolation that yielded a sufficient amount of the active agent has been too large. The screening of complex mixtures is inherently accompanied with several problems: tannins often present in ethanol extracts can cause false-positive results due to their ability to precipitate proteins; molecules in the extract mixtures can exhibit opposite activities resulting in false-negative results, and bioactive agents may be present at concentrations that are below the detection threshold for the activity screening (44).

However, the emergence of new analytical and hyphenated techniques in conjunction with advances in high-throughput screening methods revolutionized complex samples separation and processing allowing once again natural products to be actively involved in the process of drug discovery of new active agents (31, 44).

1.6 HR-BIOASSAY/HPLC-HRMS-SPE-NMR

HR-BIOASSAY/HPLC-HRMS-SPE-NMR is a bioanalytical platform that combines a high resolution microtiter plate-based bioassay with a hyphenated system that comprises high-performance liquid chromatography, high-resolution mass spectrometry, solid-phase extraction and nuclear magnetic resonance (Figure 2). This combination was proven to be extremely powerful in screening crude plant extracts since it allows pharmacological as well as chemical profiling simultaneously. The method has been already used successfully for structure elucidation of α -glucosidase inhibitors (45-50), α -amylase inhibitors (51), aldose reductase inhibitors (50), antioxidants (46, 50, 52, 53), hyaluronidase inhibitors (54), monoamine oxidase-A inhibitors (55) and PM H⁺-ATPase inhibitors (56, 57) from plant extracts, fungi and food.

In the first stage chromatographically separated fractions are subjected to a selected bioactivity test. Microtiter plates with analytes are dried before the offline assay in order to remove the chromatographic solvent and thus reducing the incompatibilities between the separation method and the bioassay (52). After overlaying the high-resolution activity profile to the HPLC trace generating the so-called biochromatogram it is possible to pinpoint individual metabolites responsible for the pharmacological activity.

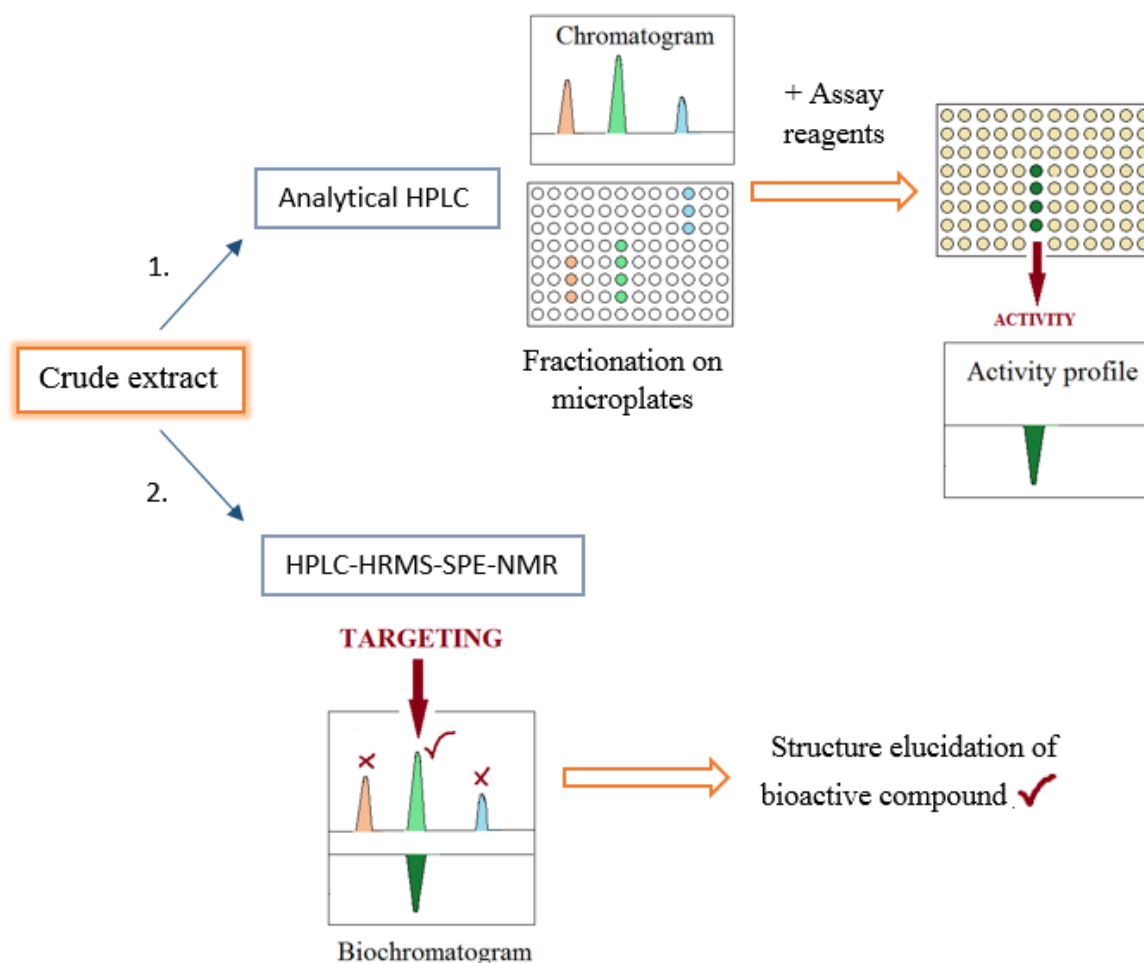


Figure 2: General workflow for identification of individual bioactive agents from plant extracts using HR-BIOASSAY/HPLC-HRMS-SPE-NMR

The aim of the second step is structure elucidation of the bioactive compound/s detected in the first part. The HPLC-HRMS-SPE-NMR system allows multiple trappings of single analytes on chosen cartridges using photodiode array (PDA) and/or MS detector to trigger the compounds of interest. Furthermore, elution into capillary NMR-tubes and the use of cryogenically cooled probe head favours structural characterization of compounds present

in limited quantities (58). The SPE step enables the selection of a desired mobile phase for the HPLC separation as there is a drying phase of cartridges with trapped compounds before eluting them into NMR tubes with a deuterated solvent and thereby avoiding the presence of signals from nondeuterated HPLC and post-column dilution solvents in NMR spectra (59). In addition a combination of HRMS and NMR spectroscopic data provides enough information for a fast dereplication and unambiguous structure elucidation (31, 60). It is also possible to upgrade the hyphenated method with circular dichroism and hence establish the absolute configuration of a selected compound. (61)

1.7 *Lophira lanceolata* Tiegh. ex Keay

1.7.1 Taxonomy

Lophira lanceolata is a flowering tree that is part of one of the most diverse families in tropical Africa. Its taxonomic classification is shown in Table I (62).

Table I: Taxonomic classification of *Lophira Lanceolata* (62)

Kingdom	Plantae
Phylum	Magnoliophyta
Class	Tracheophyta
Order	Malpighiales
Family	Ochnaceae
Genus	<i>Lophira</i>
Species	<i>Lanceolata</i>

1.7.2 Description

Lophira lanceolata is a small to medium-sized tree (Figure 3). Its final height is typically up to 16 meters. The stem is straight or twisted, its diameter reaches up to 70 cm. The bark is grey, corky and very rough flaky whereas the inner bark is yellow to brownish red. The branches angle upwards and have conspicuous leaf-scarfs. Leaves are simple and entire, they alternate but cluster at the end of branches. Stipules are 3-5 mm long and linear-lanceolate. Petiole is 2-6 cm long, blade is oblong-lanceolate, base is cuneate and often asymmetrical, apex is rounded and sometimes



Figure 3: *Lophira lanceolata* (63)

notched. The typical leaf size is 11-45 cm x 2-9 cm. When young leaves are red to bright pink. They are pinnately veined with a large number of lateral veins, clearly visible on both sides. The inflorescence is terminal, pyramidal, panicle, 15-20 cm long. Flowers are bisexual, radially symmetrical, pentamerous. They are white and scented. Pedicels are 1-1,5 cm long. The 2 outer calyx lobes are ovate-acuminate and 7–8 mm × 4–5 mm big whereas the 3 inner ones are broadly ovate and smaller (6 mm x 5 mm). The petals are free, obcordate and 17 mm x 13 mm in size. The stamens are abundant, usually in 3-5 whorls. The ovary is single-celled, superior and sessile. The fruit is conical and slightly woody. The seed's shape is ovoid and chestnut-coloured (63).

1.7.3 Habitat and geographic distribution



Figure 4: Geographic distribution of *Lophira lanceolata* (63)

Lophira lanceolata is an African tree that predominantly grows in the dry savannah areas. It is widely distributed from Senegal through the coastal countries, Central African Republic and Chad to Sudan and Uganda to the East and northern parts of Congo to the South (Figure 4). It occurs up to 1500 meters above sea level. The trees grow in groups on fallow land at the edge of forests (63).

1.7.4 Uses

Lophira lanceolata is a multipurpose tree; its wood is used for the local construction industry, as firewood and as a source of charcoal, the flowers are a source of honey and edible caterpillars are cultivated on the tree (63). However, the tree is especially valued for the edible oil extracted from its seeds. Méni oil, as the locals call it, is rich in polyunsaturated fatty acids, phytosterols, tocopherols, proteins and minerals and could therefore be exploited to overcome nutritional deficiencies in infants and children in poor countries (63-65).

The plant has a long history of use in traditional medicine. Most of its parts are exploited to treat a variety of medical conditions. Infusion of the stem bark is used as a mouthwash against toothache in Nigeria, Guinea and Mali. Young fresh or dried leaves are prepared into a drink to treat pain provoked by intestinal worms, diarrhoea and dysentery in children. Pain associated to intestinal worms can also be cured by eating directly young fresh leaves. It is also believed that a steam bath prepared from the leaves cures rheumatism and general tiredness. Syphilis, headache and hypertension are also treated with concoctions of the young red leaves (63).

1.7.5 Compounds isolated from leaves and stem bark

The compounds that have already been isolated from the stem bark and the leaves of *Lophira lanceolata* are shown in Table II and Table III.

Table II: Compounds isolated from the stem bark of *Lophira lanceolata* (63- 68)

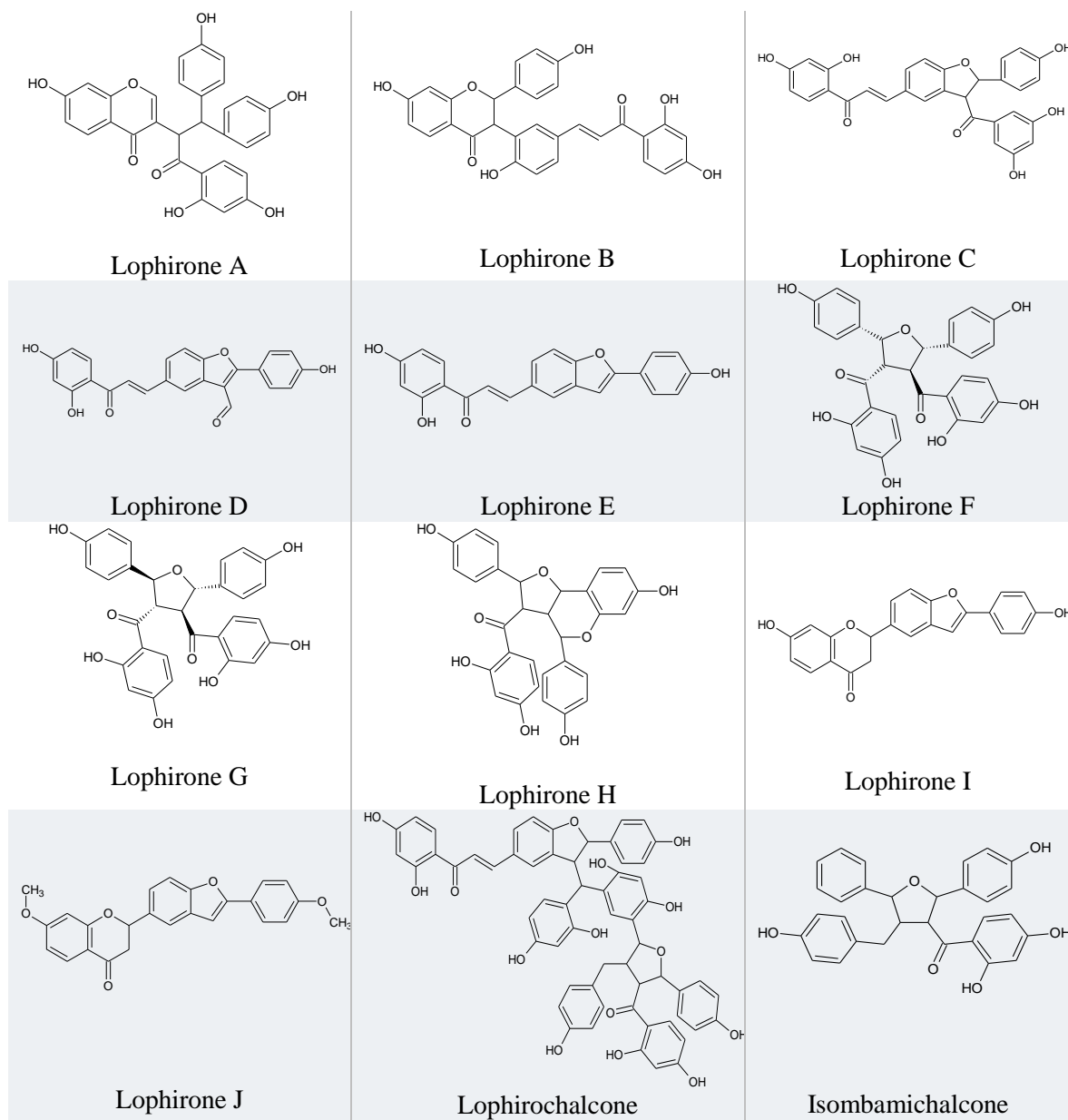
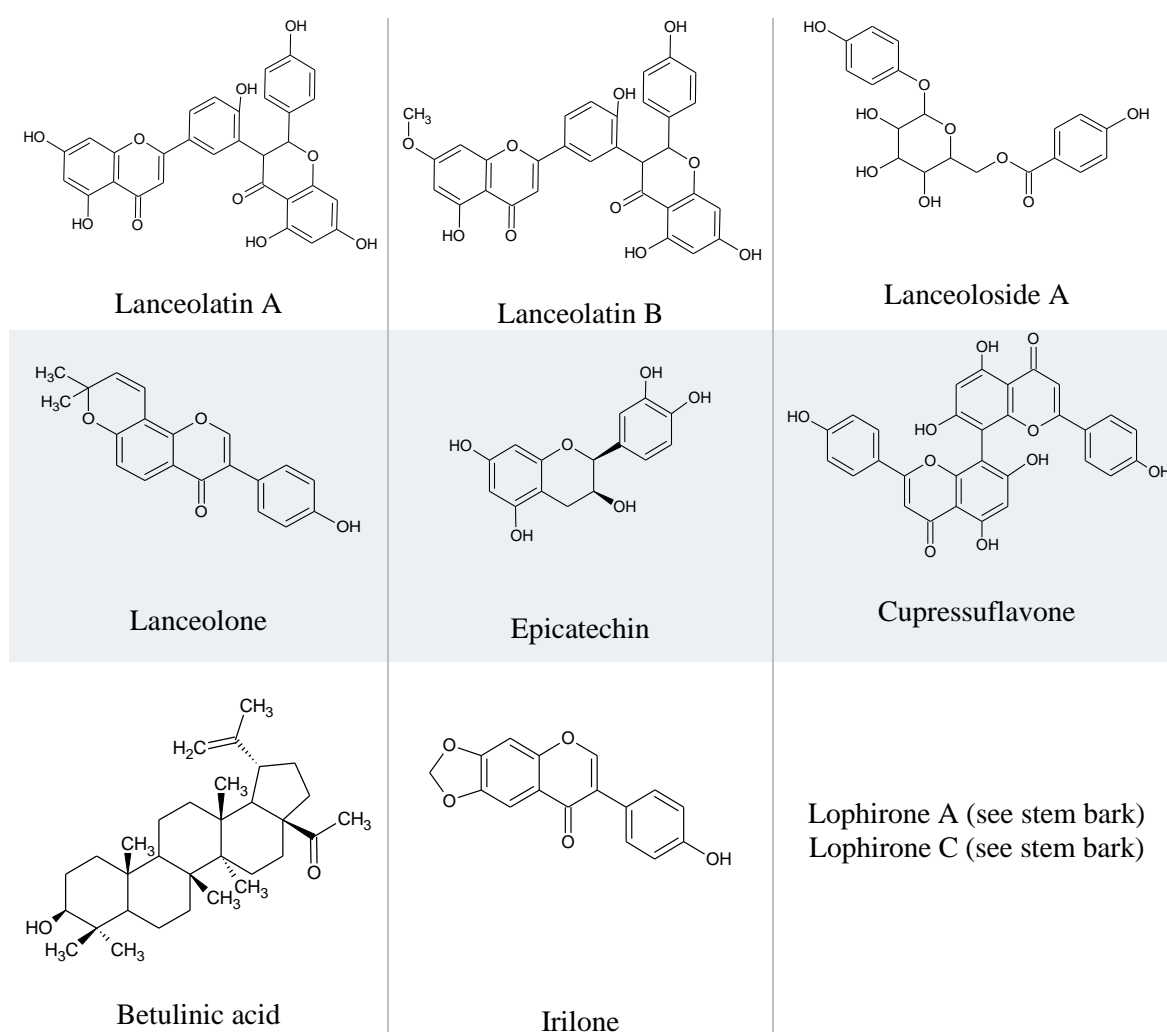


Table III: Compounds isolated from the leaves of *Lophira lanceolata* (69-73)

The extracts afforded biflavonoids (lanceolatin A, lanceolatin B (72), cupressuflavone (74)), isobiflavonoids or cleaved biflavonoids (lophirone A-E) (66-68)), tetraflavonoid (lophirochalcone) (71), chalcone dimers and cleaved chalcone dimers (lophirone F-J (69, 70), isombamichalcone (71)), an isoflavone (irilone) (76), a prenylated isoflavone (lanceolone) (73), a flavanol (epicatechin) (76), a benzoyl glucoside (lanceoloside A) (73) and a triterpenoid (betulinic acid) (75). In addition, a phytochemical screening of the leaves suggested the presence of flavonoids, anthraquinones, phenols, carbohydrates, glycosides, tannins, saponin steroids and free reducing sugars (77).

Certain lophirones have been further isolated from *Lophira alata*, the second representative of *Lophira* genus (78, 79) and from other species of the Ochnaceae family (80-83). Researchers agreed that they possess unusual skeletons and can be therefore considered markers of the Ochnaceae family (66, 82). Lanceolatin A, lanceolatin B and

isombamichalcone were so far found exclusively in *Lophira lanceolata* whereas lophirochalcone was also isolated from the stem bark of *Lophira alata* (84) and laceolone is present just in one plant belonging to the Ochnaceae family (85), *au contraire* irilone, betulinic acid, cupressuflavone and epicatechin are widely spread in several different plant species (86-91).

1.7.6 Antifungal activity

Crude extract

To date two studies suggested that *Lophira lanceolata* leaf extract has antifungal features. In a 2006 study of antimicrobial activities of medicinal plants from Cameroon it was shown that *Candida albicans* is sensitive to the methanolic leaf extract. However, the agar-dilution assay showed that its minimal inhibitory concentration (MIC) is above the highest concentration tested (1024 µg/mL). (92) In a subsequent more in-depth study an aqueous leaf extract was used and the activity against *Candida* was confirmed. In addition, activity against *Aspergillus niger* was reported. MIC and MFC (minimal fungicidal concentration) were 6.25 mg/mL for both fungi which is consistent with the first study. (93)

Compounds isolated from the stem bark and leaves

Betulinic acid was tested against *Microsporum canis*, *Candida guilliermondi*, *Sporothrix schenckii*, *Candida albicans*, *Aspergillus fumigatus*, *Cryptococcus neoformans* and *Candida spicata* showing MICs ranging from 12 to 47 µg/mL (94). Epicatechin exhibited high activity against *Aspergillus fumigatus*, *Penicillium citrii*, *Alternaria alternata*, *Macrophomina phaseolina* and *Aspergillus niger*. Using poisoned medium technique to test epicatechin at the concentration of 1000 ppm decreased fungal colony diameters by 95, 94, 90, 80 in 78 %, respectively (95). In addition epicatechin showed activity against *Candida* species (*Candida albicans* MIC=12.5 µg/ mL, MFC=50 µg/mL) (96). Cupressuflavone isolated from *Cupressocyparis leylandii* showed fungistatic activity against *Alternaria alternata*, *Fusarium avenaceum* and *Fusarium culmorum* (97).

So far no major effort was put into exploring the antifungal potential of the compounds isolated from the leaves and stem bark of *Lophira lanceolata* that are characteristic of *Lophira* genus and the Ochnaceae family. None of the compounds that have already been isolated from the leaves and stem bark of *Lophira lanceolata* were tested against the fungal PM proton pump.

2 AIM AND PLAN

PROBLEM: Fungal infections are characterized by a high incidence rate and a worldwide distribution. Despite the fact that the most frequent infections, i.e. superficial mycoses are rarely dangerous, fungi pose a significant threat to immunocompromised patients whose number is rapidly growing. Development of new antifungal agents is extremely challenging since human and fungal cells share several similarities and thus it is very demanding to ensure the appropriate selective toxicity. In addition, the emergence of new pathogenic strains rapidly changes the needs in clinical practice.

AIM: The aim of this study is to find novel compounds with antifungal properties in the stem bark and leaves of *Lophira lanceolata* Tiegh. Ex Keay, an African tree widely used in traditional medicine. To date two studies suggested that *Lophira lanceolata* leaf extract has antifungal features. However, the plant is poorly researched and its major constituents are not linked to any pharmacological activity. Our research is based on the consideration that plants are exposed to pathogenic fungi in their natural habitat and are therefore forced to synthesize antifungal secondary metabolites as defence mechanism. To evaluate the antifungal potential of isolated compounds from the plant we will use fungal PM H⁺-ATPase, a promising target for new antifungal agents.

PLAN: We will start by testing defatted ethyl acetate extracts for their ability to inhibit PM H⁺-ATPase at three different concentrations. If a crude extract shows inhibition higher than 95 % for all concentrations tested or a concentration-dependent inhibition, we will proceed with creating a high-resolution PM H⁺-ATPase inhibition profile and growth inhibition profile for *Saccharomyces cerevisiae* and *Candida albicans*. To build the profiles we will chromatographically separate the extracts into microfractions on 96-well microtiter plates and test each fraction for the PM H⁺-ATPase inhibition and growth inhibition. After overlaying the high-resolution inhibition profiles to the HPLC trace we will generate biochromatograms which will enable us to track the compounds responsible for the activity. In the following step we will try to elucidate the structures of active agents and major metabolites using a coupled method, i.e. HPLC-HRMS-SPE-NMR. We will conclude our study with a targeted isolation of compounds of interest using preparative chromatography and the assessment of IC₅₀ values for PM H⁺-ATPase, IC₅₀ values for Na⁺/K⁺-ATPase and MIC for *S. cerevisiae* and *C. albicans* for each active agent and for structurally related compounds. Figure 5 shows the expected workflow.

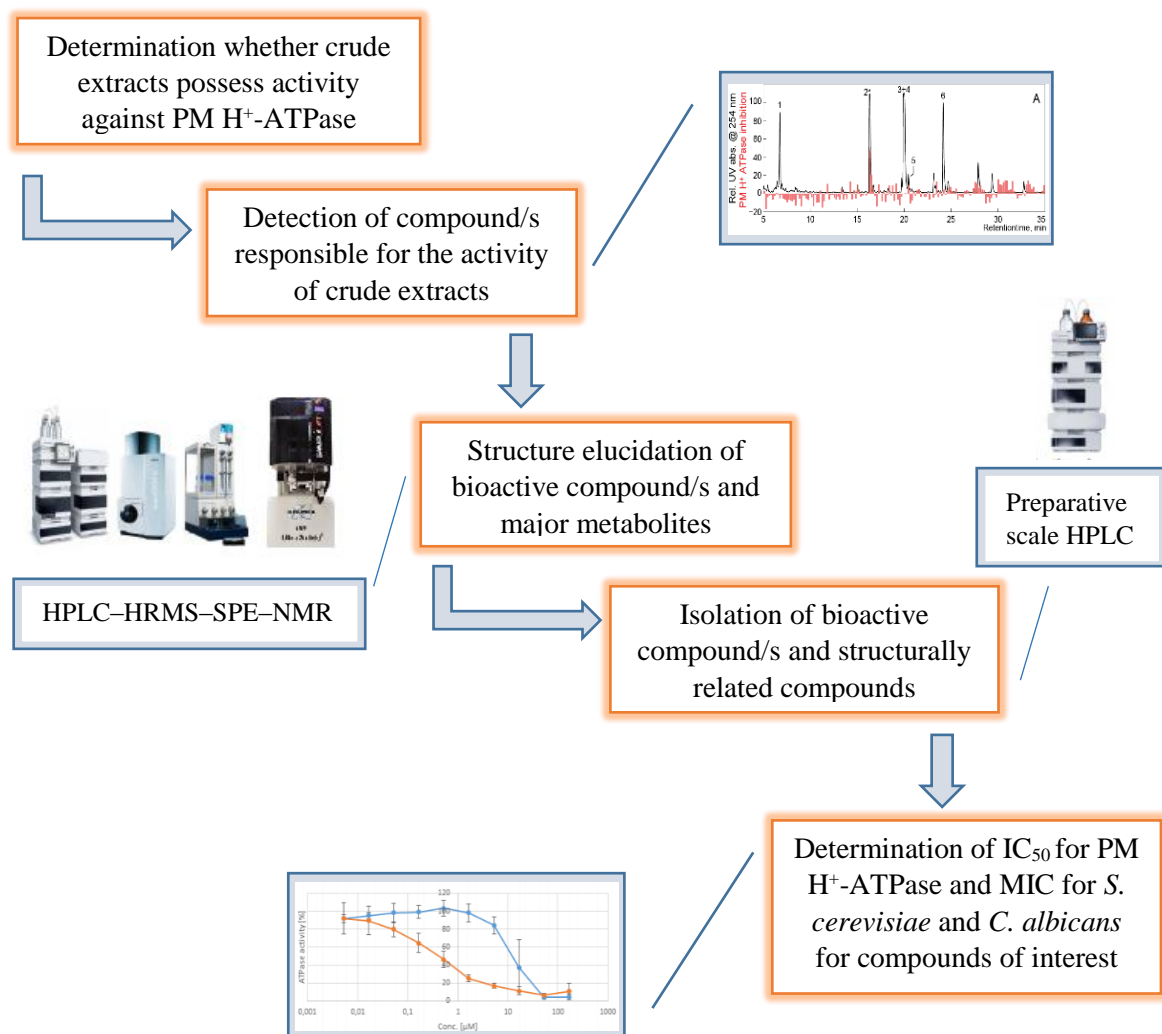


Figure 5: Expected workflow (Figures are symbolic)

3 MATERIALS AND METHODS

3.1 Materials

3.1.1 Chemicals

Reagents, solvents, analytical grade HPLC solvents, agar plates, culture media, DMSO- d_6 (99.8 atom % of deuterium), and methanol- d_4 (99.8 atom % of deuterium) were purchased from Sigma-Aldrich (St. Louis, Missouri).

Water used for HPLC was purified by deionisation and filtered through a 0.22 μm membrane (Millipore, Billerica, Massachusetts).

3.1.2 Plant material

The leaves and the stem bark of *Lophira lanceolata* Tiegh. ex Keay were collected in Ghana. After collection the plant material was airdried onsite. Voucher specimens are deposited in the Herbarium at the Department of Drug Design and Pharmacology, University of Copenhagen (Table IV).

Table IV: Plant material

Species	Plant part	Voucher
<i>Lophira lanceolata</i> Tiegh. ex Keay	leaf	PMLLL2013
<i>Lophira lanceolata</i> Tiegh. ex Keay	stem bark	PMLLB2013

3.1.3 Fungal cultures

The name, the strain designation and the manufacturer of the fungal cultures used in the study are shown in Table V.

Table V: Fungal cultures used for Growth inhibition assays

Name	Strain designation	Manufacturer
<i>Saccharomyces cerevisiae</i>	FuSc041	De Danske Gaerfabrikker, Grena, Denmark
<i>Candida albicans</i>	SC5314	LGC Standards, Boras, Sweden

3.2 Methods

3.2.1 Preparation of the Plasma Membrane H⁺-ATPase for Inhibition Assays

Plasma membrane H⁺-ATPase was prepared as previously reported (56) by PCOVERY, Copenhagen, Denmark.

3.2.2 Determination of Plasma Membrane H⁺-ATPase Activity

Determination of PM H⁺-ATPase activity was carried out as previously reported (56). The plasma membrane H⁺-ATPase activity was measured via the amount of liberated phosphate (PO₄³⁻) from the reaction that is catalysed by the enzyme (ATP + H₂O + H⁺_{in} ⇌ ADP + PO₄³⁻ + H⁺_{out}). Reactions were carried out with 2 μL sample in an assay buffer composed of 20 mM MOPS-NaOH pH 6.5, 8 mM MgSO₄, 50 mM KNO₃, 25 mM NaN₃ and 250 μM Na₂MoO₄. PM H⁺-ATPase was dissolved in the assay buffer, each well on the microtiter plate contained 2 μg of enzyme. Reactions were initiated by the addition of Na-ATP to the buffer to a final concentration of 2.5 mM and incubation for 30 min at 30 °C. We continued with the addition of STOP-solution (mixture of A, 170.3 μM C₆H₈O₆ in 0.5 M HCl; and B, 28.3 mM, (NH₄)₆Mo₇O₂₄·4H₂O in H₂O) with an incubation of 10 min at room temperature, followed by the addition of arsenite solution (154 mM NaAsO₂, 68 mM Na₃C₆H₅O₇·2H₂O, 0.35 M CH₃COOH). The amount of liberated phosphate was measured through absorbance at 860 nm after an additional incubation for 30 min at room temperature (A₈₆₀^{sample}). The maximum activity of the PM H⁺-ATPase was determined by adding 2 μL DMSO instead of the sample to the assay buffer. Thereafter we continued as described above and measured A₈₆₀^{DMSO}. A background reading of A₈₆₀ with Na-ATP and the absence of a sample and PM H⁺-ATPase was performed (A₈₆₀^{background}) in the same manner and subtracted from all the A₈₆₀ measurements.

The calculations were carried out as written below:

$$\% \text{ activity}^{\text{sample}} = 100 \% * (A_{860}^{\text{sample}} - A_{860}^{\text{background}}) / (A_{860}^{\text{DMSO}} - A_{860}^{\text{background}})$$

$$\% \text{ inhibition}^{\text{sample}} = 100 \% - \% \text{ activity}^{\text{sample}}$$

Equation 2: Calculation of % inhibition of PM H⁺-ATPase for crude extract screening and high-resolution PM H⁺-ATPase inhibition assay

3.2.3 *Candida albicans* and *Saccharomyces cerevisiae* Growth Inhibition Assay

Growth inhibition assays were performed as previously reported (56).

Frozen fungal stocks were transferred to YPD-agar plates (10 g/L yeast extract, 20 g/L glucose, 20 g/L bactopectone, 20 g/L agar) and incubated at 30 °C overnight. Cells were suspended in sterile H₂O and the start optical density, measured at 600 nm (OD₆₀₀) was adjusted to *C. albicans* OD₆₀₀=0.025 and *S. cerevisiae* OD₆₀₀=0.05. 3 µL of plant sample, 100 µL of fungal cell suspension and 97 µL of 2 X RPMI-medium (20.8 g/L RPMI-1640 medium, 36 g/L glucose, 0.33 M MOPS) were transferred into a microtiter plate and incubated for 24 h at 30 °C. OD measurements were carried out at 490 nm. The maximum growth (0 % inhibition) was determined by adding 3 µL of DMSO instead of the sample and thereafter continued in the same manner as described above (OD₄₉₀^{DMSO}). The OD₄₉₀ of the culture medium was measured (OD₄₉₀^{background}).

The calculations were carried out as written below:

$$\% \text{ growth}^{\text{sample}} = 100 \% * (\text{OD}_{490}^{\text{sample}} - \text{OD}_{490}^{\text{background}}) / (\text{OD}_{490}^{\text{DMSO}} - \text{OD}_{490}^{\text{background}})$$

$$\% \text{ inhibition}^{\text{sample}} = 100 \% - \% \text{ growth}^{\text{sample}}$$

Equation 3: Calculation of % growth inhibition of Candida albicans and Saccharomyces cerevisiae for high-resolution growth inhibition assay

3.2.4 Extractions

For Crude extract screening

0.3 g of grinded plant material was extracted with 3.6 mL of ethyl acetate by sonication for 2 h. The extracts were filtered (Q-Max RR 13 mm 0.45 µm Nylon, Frisenette, Denmark) and the solvent was evaporated to dryness *in vacuo* at temperatures below 40 °C. Extracts were dissolved in 2 mL of 90 % aqueous methanol and defatted (fats removed) by partitioning with 1.5 mL of petroleum ether (b.p. 40-65 °C). The petroleum ether fraction was discarded and the 90 % aqueous methanol phase was evaporated to dryness *in vacuo* at temperatures below 40 °C.

For High-Resolution screening and HPLC-HRMS-SPE-NMR

Grinded plant material (3 g leaves, 50 g stem bark) was extracted with 40 mL and 500 mL of ethyl acetate, respectively, by sonication for 2 h. The extracts were filtered (Q-Max RR

25 mm 0.45 μm Nylon, Frisette, Denmark) and the solvent was evaporated to dryness *in vacuo* at temperatures below 40 °C. The leaf extract was dissolved in 50 mL of 90 % aqueous methanol and defatted by triple partitioning with 40, 30 and 20 mL of petroleum ether (b.p. 40-65 °C). The stem bark extract was dissolved in 150 mL of 90 % aqueous methanol and defatted by triple partitioning with 115, 85, 60 mL of petroleum ether (b.p. 40-65 °C). The petroleum ether fraction was discarded and the 90 % aqueous methanol phase was evaporated to dryness *in vacuo* at temperatures below 40 °C. Leaf and bark extracts were dissolved in methanol at the final concentration of 30 mg/mL for both high-resolution PM H^+ -ATPase inhibition assay and HPLC-HRMS-SPE-NMR analyses.

For Preparative-scale isolation

For preparative-scale isolation of selected metabolites an additional 35 g of grinded leaves were extracted with 450 mL ethyl acetate by sonication for 2 hours. The extracts were filtered (Q-Max RR 25 mm 0.45 μm Nylon, Frisette, Denmark) and the solvent was evaporated to dryness *in vacuo* at temperatures below 40°C. The extract was dissolved in 180 mL of 90 % aqueous methanol and defatted by triple partitioning with 135, 100 and 70 mL of petroleum ether (b.p. 40-65 °C). The petroleum ether fraction was discarded and the 90 % aqueous methanol phase was evaporated to dryness *in vacuo* at temperatures below 40 °C. The extract was dissolved in methanol at the final concentration of 65 mg/mL. For preparative scale isolation of selected metabolites from the stem bark we used the extract obtained in 3.2.4.2. After the high-resolution PM H^+ -ATPase inhibition assay and HPLC-HRMS-SPE-NMR analyses the solvent was removed to dryness using nitrogen and re-dissolved in methanol to the final concentration of 35 mg/mL.

3.2.5 Crude extract screening for PM H^+ -ATPase inhibition

0.3 g of grinded plant material was extracted as described in 3.2.4.1. The total amount of the dry material obtained with the extraction was dissolved in 100 μL of DMSO to gain a solution of an unknown concentration c . The solution of concentration c was diluted with DMSO in a ratio 1:1 to form a solution of concentration $c/2$. The solution of concentration $c/2$ was diluted with DMSO in a ratio 1:1 to form a solution of concentration $c/4$. All three solutions were tested for PM H^+ -ATPase inhibition. The assay was performed in duplicate for each concentration according to the protocol described in 3.2.2.

3.2.6 High-Resolution PM H⁺-ATPase Inhibition Assay and Growth Inhibition Assay

Chromatographic separation of defatted extract of *Lophira lanceolata* leaves and stem bark was performed with an Agilent 1200 series instrument (Santa Clara, CA) consisting of a quaternary pump, a degasser, a thermostated column compartment, a photodiode-array detector, a high-performance auto sampler and a fraction collector, all controlled by Agilent ChemStation ver. B.03.02 software and equipped with a reversed phase Luna C₁₈(2) column (Phenomenex, 150 × 4.6 mm, 3 μm, 100 Å) maintained at 40 °C. The aqueous eluent (A) consisted of water/acetonitrile (95:5, v/v) and the organic eluent (B) consisted of water/acetonitrile (5:95, v/v); both acidified with 0.1 % formic acid. The eluent flow rate was maintained at 0.5 mL/min with the following elution profile: 0 min, 10 % B; 30 min, 100 % B; 35 min, 100 % B, with 10 min equilibration prior to injection of 10 μL defatted extract (30 mg/mL). The column eluent was directed to an automated fraction collector and eluent in a 30 min window were collected in 88 μL aliquots in 160 wells of two 96-well V-shaped microtiter plates (Brand, Wertheim, Germany) (excluding outer columns), concentrated *in vacuo* and redissolved in 30 μL DMSO. From each well 3 × 2 μL and 3 × 3 μL were used for the PM H⁺-ATPase inhibition assays and the growth inhibition assays, respectively, in triplicate as described above.

3.2.7 HPLC-HRMS-SPE-NMR

The HPLC-HRMS-SPE-NMR system consisted of an Agilent 1200 chromatograph comprising quaternary pump, degasser, thermostated column compartment, auto sampler, and photodiode array detector (Santa Clara, CA), a Bruker micrOTOF-Q II mass spectrometer (Bruker Daltonik, Bremen, Germany) equipped with an electrospray ionization source and operated via a 1:99 flow splitter, a Knauer Smartline 120 pump for post-column dilution (Knauer, Berlin, Germany), a Spark Holland Prospekt2 SPE unit (Spark Holland, Emmen, The Netherlands), a Gilson 215 liquid handler equipped with a 1-mm needle for automated filling of 1.7-mm NMR tubes, and a Bruker Avance III 600 MHz NMR spectrometer (¹H operating frequency 600.13 MHz) equipped with a Bruker SampleJet sample changer and a cryogenically cooled gradient inverse triple-resonance 1.7-mm TCI probe-head (Bruker Biospin, Rheinstetten, Germany). Mass spectra were acquired in positive ionization mode, using drying temperature of 200 °C, capillary voltage of 4100 V, nebulizer pressure of 2.0 bar, and drying gas flow of 7 L/min. A solution of sodium formate

clusters was automatically injected in the beginning of each run to enable internal mass calibration. Cumulative SPE trapping of *L. lanceolata* leaf and stem bark extracts was performed after 10 consecutive separations using optimized chromatographic methods for leaf and stem bark extracts, as follows. *Leaves*: 0 min., 20 % B; 10 min., 40 % B; 40 min., 45 % B; 60 min., 60 % B; 61 min., 100 % B; 75 min., 100 % B; *Bark*: 0 min., 10 % B; 30 min., 100 % B; 35 min., 100 % B. Both with 10 min. equilibration prior to injection of 20 μ L defatted extract (30 mg/mL). The HPLC eluate was diluted with Milli-Q water at a flow rate of 1.0 mL/min prior to trapping on 10 \times 2 mm i.d. Resin GP (general purpose, 5-15 μ m, spherical shape, polydivinyl-benzene phase) SPE cartridges from Spark Holland (Emmen, The Netherlands), and analytes were trapped using thresholds of the HPLC UV-trace at 254 and 280 nm. Loaded cartridges were dried with pressurized nitrogen gas for 45 min each prior to elution with methanol-*d*₄. Separations were controlled by Bruker Hystar version 3.2 software, automated filling of NMR tubes was controlled by PrepGilsonST version 1.2 software, and automated NMR acquisition was controlled by Bruker IconNMR version 4.2 software.

3.2.8 Preparative scale isolation of selected metabolites

Compounds **2**, **3**, **4**, **6**, and **8** were isolated on an Agilent 1100 preparative-scale HPLC (Santa Clara, CA) consisting of two preparative solvent delivery units, a multiple wavelength detector, an autosampler, and an optional fraction collector. Separation was performed on a Luna C₁₈(2) column (Phenomenex, 250 \times 21.2 mm, 5 μ m, 100 Å) operated at room temperature at a flow-rate of 20 mL/min. The leaves were separated using the same chromatographic method as in the HPLC-HRMS-SPE-NMR analysis whereas the method for the stem bark was optimized, as follows: 0 min, 10 % B; 60 min, 70 % B; 80 min, 100 % B; 90 min, 100 % B. Three injections of 900 μ L (concentration = 65 mg/mL in methanol) of the leaf extract and two injections of 450 μ L (concentration = 35 mg/mL in methanol) of the stem bark extract underwent preparative chromatography. Peaks were collected manually following absorbance profile 280 nm. Chromatographic solvent was evaporated using a centrifugal evaporator.

3.2.9 NMR Experiments

All NMR spectra were recorded in methanol-*d*₄ or DMSO-*d*₆ at 300 K. ¹H and ¹³C chemical shifts were referenced to the residual solvent signal (δ_{H} 3.31 and δ_{C} 49.00 for methanol-*d*₄

and δ_{H} 2.50 and δ_{C} 39.52 for DMSO-*d*₆). (98) One-dimensional ¹H NMR spectrum was acquired in automation (temperature equilibration to 300 K, optimization of lock parameters, gradient shimming, and setting of receiver gain) with 30°-pulses, 3.66 s inter-pulse intervals, 64k data points and multiplied with an exponential function corresponding to line-broadening of 0.3 Hz prior to Fourier transform. Phase-sensitive DQF-COSY and NOESY spectra were recorded using a gradient-based pulse sequence with a 20 ppm spectral width and 2k x 512 data points (processed with forward linear prediction to 1k data points). Multiplicity-edited HSQC spectrum was acquired with the following parameters: spectral width 20 ppm for ¹H and 200 ppm for ¹³C, 2k x 256 data points (processed with forward linear prediction to 1k data points), and 1.0 s relaxation delay. HMBC spectrum was optimized for ⁿJ_{C,H} = 8 Hz and acquired using the following parameters: spectral width 20 ppm for ¹H and 240 ppm for ¹³C, 2k x 128 data points (processed with forward linear prediction to 1k data points), and 1.0 s relaxation delay. NMR data processing was performed using ACDLABS 12.0 software. The structures of the compounds were drawn using ChemBioDraw Ultra 14.0 software.

3.2.10 Determination of IC₅₀ values for PM H⁺-ATPase, IC₅₀ values for Na⁺/K⁺-ATPase and MIC for 50 % growth inhibition of *S. cerevisiae* and *C. albicans*

Determination of IC₅₀ values for PM H⁺-ATPase, IC₅₀ values for Na⁺/K⁺-ATPase and MIC for 50 % growth inhibition of *S. cerevisiae* and *C. albicans* was performed by PCOVERY, Copenhagen, Denmark.

Compounds **2**, **3** and **8**, isolated by preparative chromatography, were dissolved in DMSO at the final concentration of 10 mM for assessment of IC₅₀ values against PM H⁺-ATPase, IC₅₀ values for the inhibition of Na⁺/K⁺ ATPase and MIC for 50 % inhibition of fungal growth tested on *Saccharomyces cerevisiae* and *Candida albicans*. Determination of IC₅₀ was performed in triplicate, while the MIC determination was performed in duplicate.

4 RESULTS AND DISCUSSION

4.1 Extractions

Defatted ethyl acetate extracts of both leaves and stem bark of *Lophira lanceolata* were tested for their ability to inhibit PM H⁺-ATPase as part of a larger screening campaign investigating the antifungal potential of African medicinal plants. The extraction method in the proof-of-concept project was simple, quick and was proved to be powerful. However, some ethanol extracts contained tannins, which have the ability to precipitate proteins and thus lead to false positive results in PM H⁺-ATPase inhibition testing (56). Since it was previously demonstrated that the leaves of *Lophira lanceolata* contain tannins (77) we could not use the extraction solvents (acetone, ethanol and methanol) previously used for phytochemical screenings of the leaves and the stem bark (66-77). These solvents possess a high polarity index and are therefore inappropriate for the extraction of plant material that is subsequently tested for the PM H⁺-ATPase inhibition. To prevent the extraction of tannins we chose a less polar menstruum, i.e. ethyl acetate which is also easy to remove (99). Ethyl acetate extractions were successful as we extracted compounds which were previously isolated from the plant but also four new compounds that have never been isolated from the plant before. Since we found inhibitors of the PM H⁺-ATPase in ethyl acetate extracts, we decided not to prepare and test extracts from solvents with a higher or lower polarity which could have been however interesting.

The volumes of the solvents used were proportionally adjusted to the quantity of the starting dry plant material. The partitioning between 90 % aqueous methanol and petroleum ether was performed three times in order to remove completely the lipid constituents, especially the chlorophylls in the leaves that might interfere in further steps. Defatting of the stem bark is usually not necessary (99). We decided to perform it to keep the extraction process for the leaves and the stem bark the same.

On average the extractions afforded 591.3 mg of extract/100 g of leaves and 125.6 mg of extract/100 g stem bark.

4.2 Crude extract screening for PM H⁺-ATPase inhibition

In the first stage of our study we tested the defatted ethyl acetate extracts from the leaves and the stem bark of *Lophira lanceolata* for their ability to inhibit PM H⁺-ATPase. For the initial screening we extracted 0.3 g of plant material as we were aiming to discover

compounds that are sufficiently potent to exhibit their inhibitory activity at relatively low concentrations (56). The extract was prepared in three concentrations in order to observe the relationship between activity and concentration. The inhibition rate of PM H⁺-ATPase was determined by measuring the amount of liberated phosphate from the ATP hydrolysis reaction (Equation 1). The assay was carried out as described in 3.2.2. The percentage of inhibition of the PM H⁺-ATPase exhibited by the extracts was calculated as shown in equation 2. The results are displayed in table VI.

Table VI: Crude extract screening for PM H⁺-ATPase inhibition. Average inhibition of duplicates along with its respective standard deviation are given.

Sample	Concentration	Inhibition (%) ^a
Leaf	c	88 ± 3.5
	c/2	84 ± 7.8
	c/4	72 ± 1.4
Stem bark	c	97 ± 7.8
	c/2	82 ± 9.9
	c/4	67 ± 7.8

^an=2

The standard deviations of the inhibitions are relatively high, especially for the stem bark extract (7.8 – 9.9). In addition, the inhibition rate for one measurement of the stem bark extract with concentration c was above 100 %, i.e. 102 % (not show in the table). Nevertheless, the aim of the screening was to determine whether crude extracts possess the ability to inhibit the PM H⁺-ATPase. In accordance with a previous study (56), we decided that the extracts worth investigating are the ones showing over 95 % inhibition for all concentrations tested or a concentration-dependent activity profile. *Lophira lanceolata* leaf and stem bark extract clearly show a concentration-dependent activity profile as seen in Figure 6. Consequently, we proceeded with the high-resolution inhibition assays.

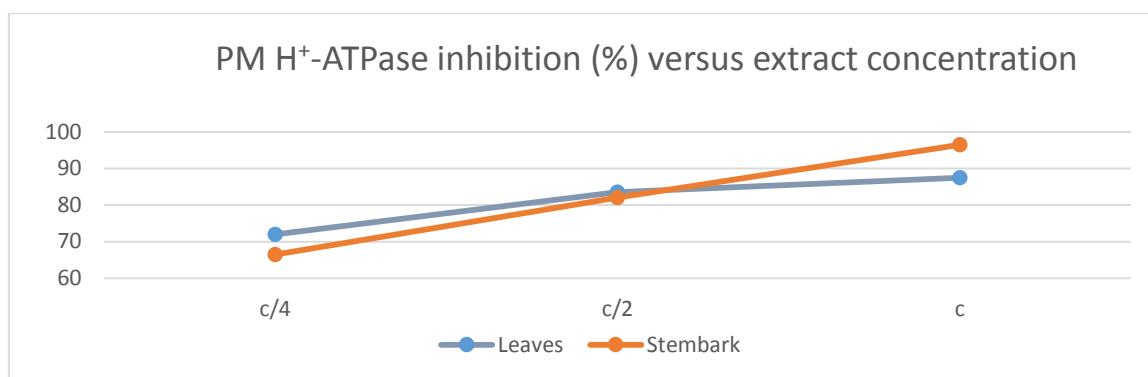


Figure 6: PM H⁺-ATPase inhibition profile versus concentration for crude extracts

4.3 High-Resolution Inhibition Assays

The purpose of the high-resolution inhibition assays was to pinpoint the metabolite/s responsible for the activity exhibited by the extracts in the initial screening. The HPLC method allowed a fairly well separated chromatographic peaks in the UV-trace at 254 nm. The eluate from 5-35 min (leaves) and 4-34 min (stem bark) was collected in two 96 well microtiter plates, using 160 wells in total, yielding fractions of 88 μ L and a resolution of 5.3 data points/min. The chromatographic solvent from each well was evaporated, and the dried material was reconstituted in DMSO. Every microfraction was tested for its *in vitro* inhibitory effects on the PM H⁺-ATPase enzyme and for growth inhibition of *C. albicans* and *S. cerevisiae*.

4.3.1 PM H⁺-ATPase Inhibition Assay

The principle and the execution of the PM H⁺-ATPase inhibition assay was identical to the crude extract screening described in 3.2.2. The % of inhibition of PM H⁺-ATPase of each well was plotted against its respective retention time to create the so-called high-resolution PM H⁺-ATPase inhibition profiles. After overlaying the PM H⁺-ATPase inhibition profile to the HPLC UV-trace at 254 nm (Figure 7 and 8) it was clear that peak **2** from the leaf extract and peak **8** from stem bark extract correlated with PM H⁺-ATPase inhibition and were therefore responsible for the crude extracts' activity observed in the first step of our study.

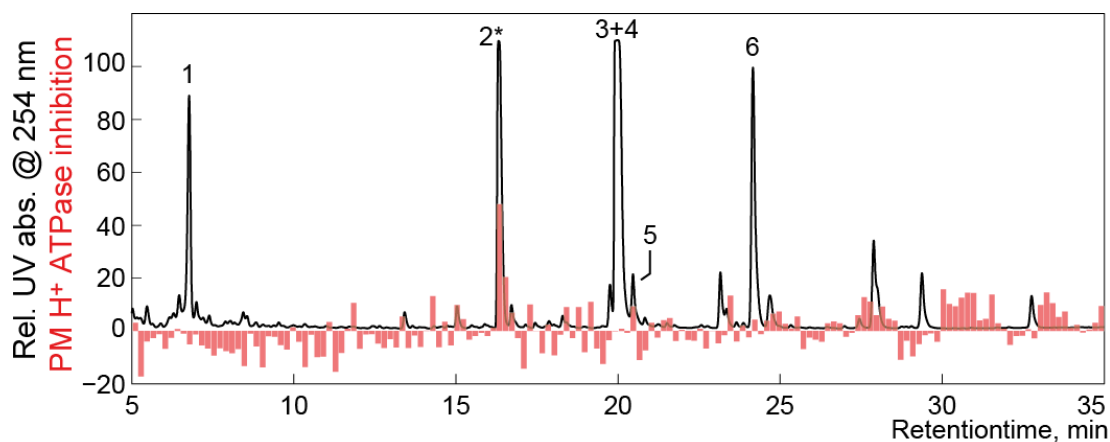


Figure 7: HPLC chromatogram at 254 nm (black) overlaid by plasma membrane H^+ -ATPase inhibition profile (red bars) of *L. lanceolata* leaf extract.

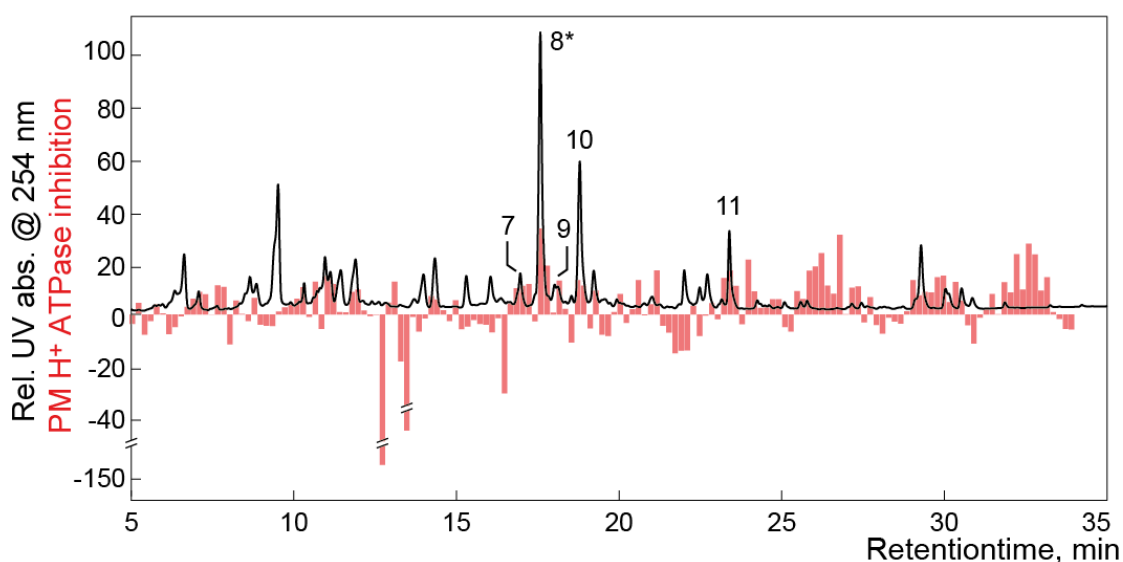


Figure 8: HPLC chromatogram at 254 nm (black) overlaid by plasma membrane H^+ -ATPase inhibition profile (red bars) of *L. lanceolata* stem bark extract.

Thus, our main focus in the HPLC-HRMS-SPE-NMR stage was going to be structure elucidation of compounds **2**, **8** and of the metabolites with molecular masses similar to the ones of the active compounds

4.3.2 *C. albicans* and *S. cerevisiae* Growth Inhibition Assay

To determine the extent of growth inhibition of selected fungal cultures exhibited by singular microfractions we followed the procedure described in 3.2.3. The percentage of inhibition of growth of *C. albicans* and *S. cerevisiae* was calculated using the equation 3. The % of

inhibition of fungal growth of each well was plotted against its respective retention time to create the so-called high-resolution *C. albicans* and *S. cerevisiae* growth inhibition profiles. After overlaying the growth inhibition profiles to the HPLC UV-trace at 254 nm (Figures 9-12) we could conclude that none of the major metabolites was strongly nor unambiguously correlated to *C. albicans* or *S. cerevisiae* growth inhibition.

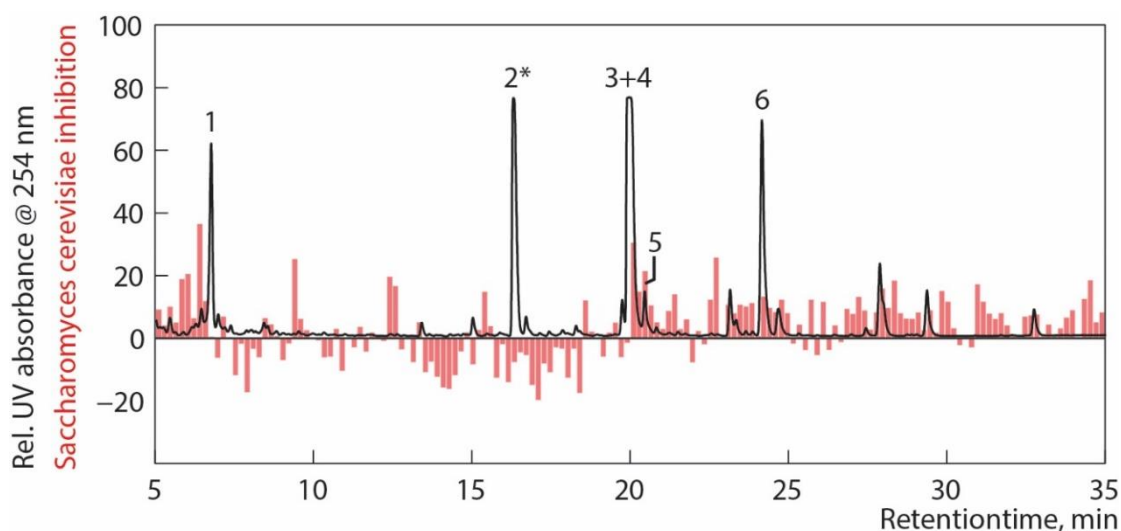


Figure 9: HPLC chromatogram at 254 nm (black) overlaid by *Saccharomyces cerevisiae* growth inhibition profile (red bars) of *L. Lanceolata* leaf extract

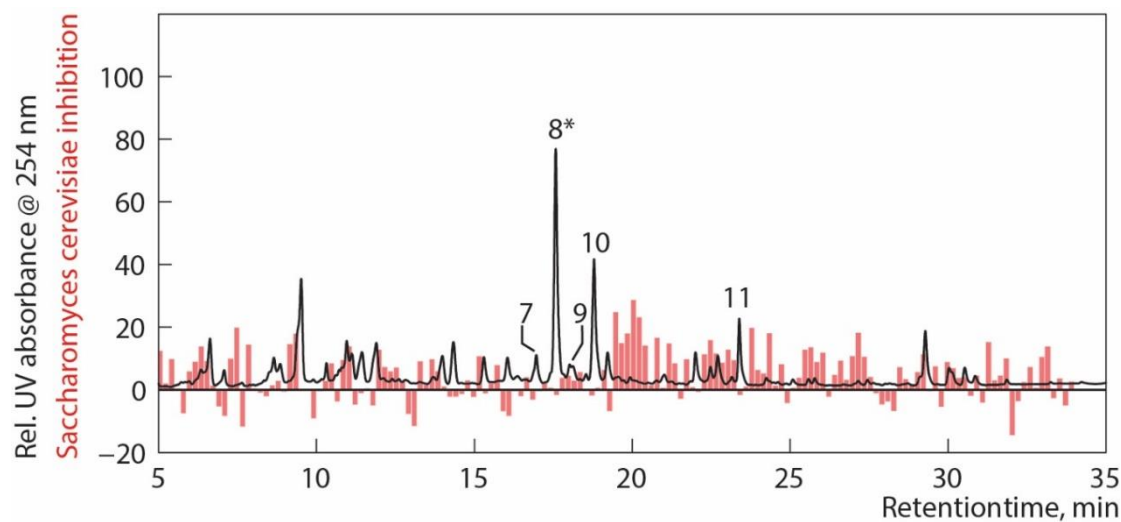


Figure 10: HPLC chromatogram at 254 nm (black) overlaid by *Saccharomyces cerevisiae* growth inhibition profile (red bars) of *L. Lanceolata* stem bark extract.

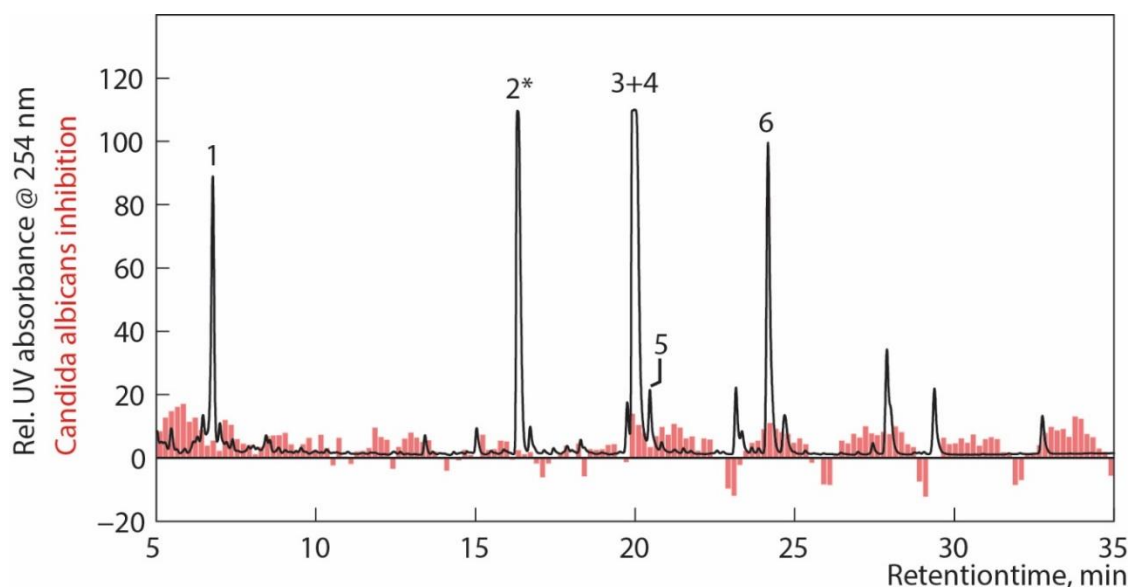


Figure 11: HPLC chromatogram at 254 nm (black) overlaid by *Candida albicans* growth inhibition profile (red bars) of *L. Lanceolata* leaf extract.

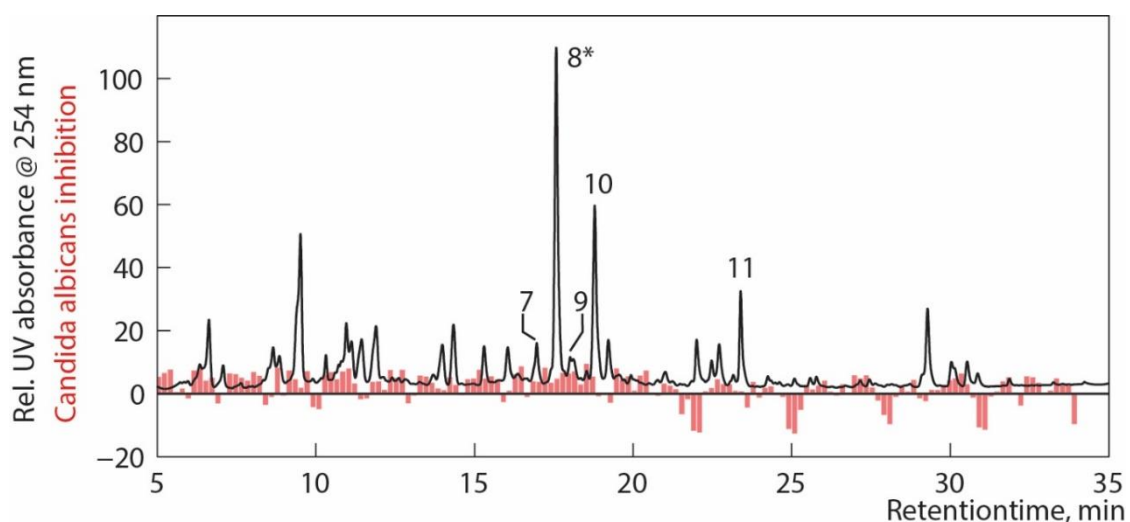


Figure 12: HPLC chromatogram at 254 nm (black) overlaid by *Candida albicans* growth inhibition profile (red bars) of *L. Lanceolata* stem bark extract.

4.3.3 Comment on High-resolution screening

All of the biochromatograms displayed anomalies. The measured absorbance and optical density for certain microfractions was lower than the corresponding blank, which resulted in negative readings. Additionally, in retention time ranges where no major components elute, it was possible to observe an apparent inhibition of the enzyme and/or fungal growth. The

distorted results were linked to the precipitation or intense coloration of some samples in addition to the occurrence of air bubbles. However, the aim of this step was to pinpoint the metabolites responsible for the activity of the crude extracts. Peak **2** from the leaf extract and peak **8** from the stem bark extract showed a clear correlation with the PM H⁺-ATPase inhibition. Besides, the activity of these compounds was significantly higher in comparison to the activity exhibited by other major metabolites. On the other hand, none of the peaks showed a correlation with *S. cerevisiae* or *C. albicans* growth inhibition. *C. albicans* growth inhibition profiles displayed a systematic error, evident from the recurrence of the same pattern of measured inhibitions in equal time intervals throughout the entire test time frame. The decision not to repeat the tests was adopted mainly because we focused on finding inhibitors of fungal PM H⁺-ATPase enzyme. The discovery of compounds that at the same time suppress the growth of *C. albicans* and/or *S. cerevisiae* would be however advantageous. Nevertheless, for the agents that showed inhibition of fungal PM H⁺-ATPase we decided to determine the MIC values against *C. albicans* and *S. cerevisiae* in the last part of our study.

4.4 HPLC-HRMS-SPE-NMR

Before proceeding with the HPLC-HRMS-SPE-NMR step, the analytical scale HPLC method for *Lophira lanceolata* leaves was optimized in order to allow better separation of compounds **3** and **4**. It was previously shown that a detailed phytochemical analysis is beneficial for the understanding of the structure-activity relationship (57), therefore we decided to investigate not only the two active compounds (**2** and **8**) but also the metabolites with similar molecular masses as these were likely to be related to the active compounds. The analytical scale HPLC method for *Lophira lanceolata* stem bark stayed the same as for the high-resolution PM H⁺-ATPase inhibition assay and growth inhibition assay since it allowed a good separation of major metabolites.

Figures 13 and 14 show the UV chromatogram at 254 nm used for HPLC-HRMS-SPE-NMR analyses with peak numbers corresponding to those indicated in Figures 7 and 8 based on HRMS analyses.

HPLC-HRMS-SPE-NMR was proven successful for fast and efficient chemical analysis of metabolites of *Lophira lanceolata* leaves and stem bark. The only issue we encountered was poor solubility of compounds **4** and **6** in the selected NMR solvent resulting in low S/N ratios in the NMR spectra. Since the method is coupled it was not possible to monitor the

performance of each step and thus, it was impossible to observe the insolubility issue before the preparative scale isolation of the compounds.

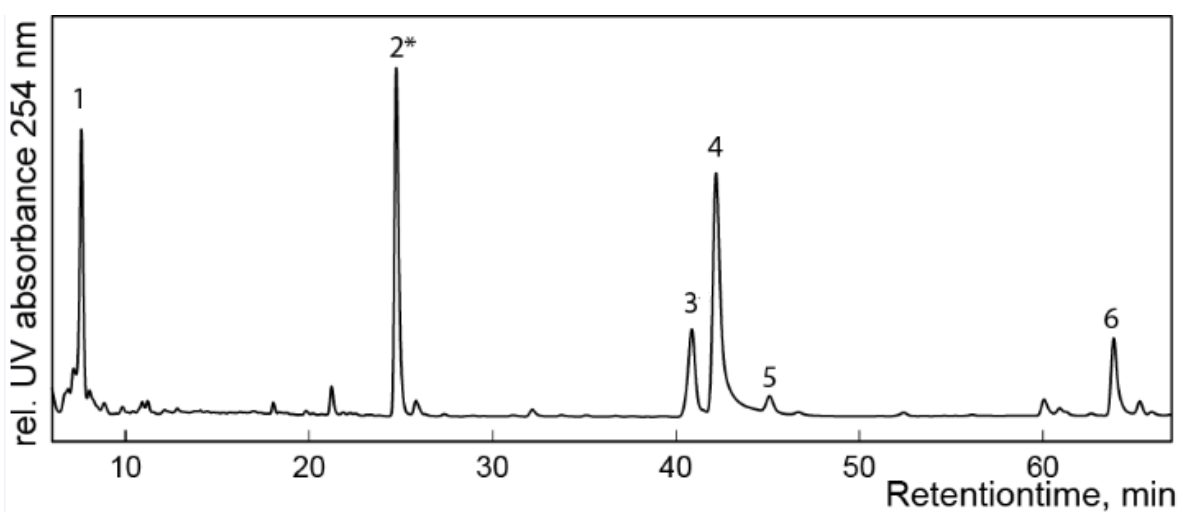


Figure 13: HPLC chromatogram at 254 nm for leaf extract, used for HPLC-HRMS-SPE-NMR analysis. Peaks numbered 1-6 correspond to compounds 1-6.

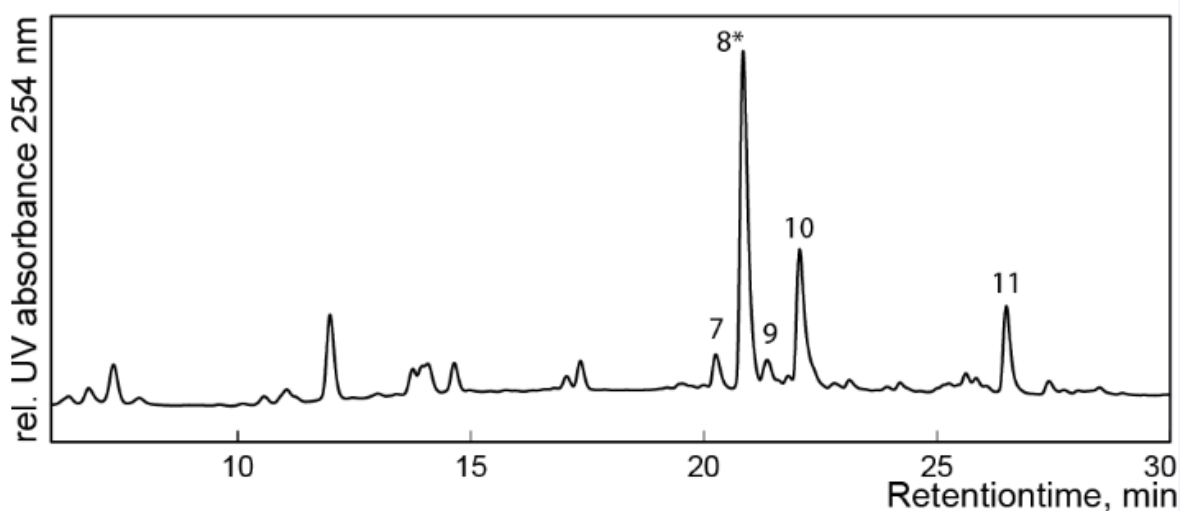


Figure 14: HPLC chromatogram at 254 nm for stem bark extract, used for HPLC-HRMS-SPE-NMR analysis. Peaks numbered 7-11 correspond to compounds 7-11.

4.5 Preparative scale isolation

For the means of the preparative scale isolation the leaf extract was separated using the same chromatographic method as in the HPLC-HRMS-SPE-NMR analysis whereas the method for the stem bark was optimized in order to facilitate the manual collection of peaks of interest. The active agents 2 and 8 pinpointed by the high-resolution H⁺-ATPase bioassay

together with compound **3** due to structural similarities with **2** were isolated for further investigation on their antifungal properties. In addition, compound **4** and **6** were also isolated as the S/N ratios observed in the NMR spectra acquired with HPLC-HRMS-SPE-NMR were low compared to the amount indicated by their UV absorbance. After evaporating the chromatographic solvent and trying to dissolve isolated compounds **4** and **6** in methanol-*d*₄, the solvent used for the elution of trapped metabolites in the NMR tubes, we could confirm that low S/N ratios in the NMR spectra acquired with HPLC-HRMS-SPE-NMR were due to insolubility of the compounds in methanol-*d*₄. For further NMR experiments compounds **4** and **6** were dissolved in DMSO-*d*₆. Table VII shows the amounts of isolated compounds using preparative isolation chromatography. The purity of all isolated peaks was >95 % (assessed by HPLC-PDA-HRMS).

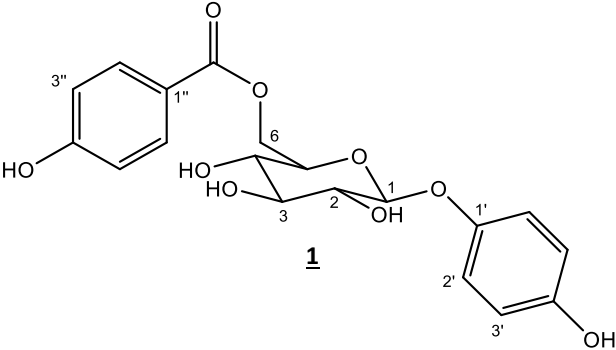
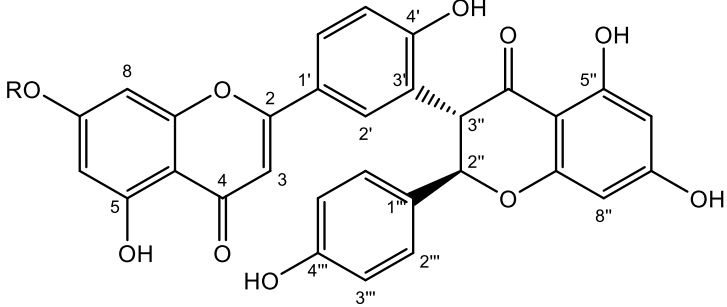
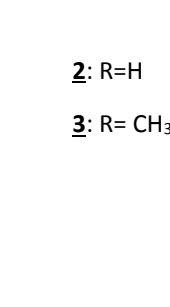
Table VII: Amounts of isolated compounds using preparative scale isolation

Compound number	2	3	4	6	8
Weight [mg]	15.8	4.7	7.5	1.8	3.7

4.6 NMR experiments

For an unambiguous structure elucidation compounds **1-11** underwent a detailed HRMS, ¹H NMR and 2D NMR (DQF-COSY, NOESY, HSQC and HMBC) analysis. NMR spectra for compounds **1 – 3, 5, 7 – 11** were recorded in methanol-*d*₄ in HPLC-HRMS-SPE-NMR, whereas NMR spectra for compounds **4** and **6** were recorded in DMSO-*d*₆ after being isolated by preparative scale HPLC. Retention time, MS and ¹H NMR data obtained with HPLC-HRMS-SPE-NMR and ¹H NMR data obtained after preparative scale isolation of **4** and **6** are shown in Table VIII.

Table VIII: Peak number, name, structure, retention time, MS and ^1H NMR data obtained with HPLC-HRMS-SPE-NMR (methanol- d_4) for 1, 2, 3, 5, 7, 8, 9, 10, 11 and ^1H NMR data obtained after preparative scale isolation of 4 and 6 (DMSO- d_6)

Peak	<u>1</u>	<u>2</u>	<u>3</u>
Name	Lanceoloside A	Lanceolatin A	Lanceolatin B
Structure			
RT (min)	7.59	24.76	40.86
m/z (MF, ppm)	393.1158 $[\text{M}+\text{H}]^+$ ($\text{C}_{19}\text{H}_{21}\text{O}_9^+$, ΔM 5.9)	541.1114 $[\text{M}+\text{H}]^+$ ($\text{C}_{30}\text{H}_{21}\text{O}_{10}^+$, ΔM 2.9)	555.1263 $[\text{M}+\text{H}]^+$ ($\text{C}_{31}\text{H}_{23}\text{O}_{10}^+$, ΔM 4.8)
^1H NMR ((nH, m, J (in Hz))	7.90 (2H, AA', H-2''/H-6''), 6.94 (2H, AA', H-3'/H-5'), 6.86 (2H, XX', H-3''/H-5''), 6.61 (2H, XX', H-2'/H-6'), 4.73 (1H, d, 7.4 Hz, H-1), 4.67 (1H, dd, 11.8, 2.2 Hz, H-6b), 4.35 (1H, dd 11.8, 7.5 Hz, H-6a), 3.70 (1H, ddd, 9.7, 7.5, 2.2 Hz, H-5), 3.46 (2H, ABC system, H-3 and H-2), 3.42 (1H, ABC system, H-4)	7.68 (1H, dd, 8.3, 1.4 Hz, H-6'), 7.44 (1H, d, 1.4 Hz, H-2'), 7.17 (2H, AA', H-2'''/H-6'''), H-2'''/H-6'''), 6.86 (1H, d, 8.3 Hz, H-5'), 6.65 (2H, XX', H-3'''/H-5'''), 6.44 (1H, s, H-3), 6.41 (1H, d, 1.9 Hz, H-8), 6.19 (1H, d, 1.9 Hz, H-6), 5.95 (1H, d, 2.2 Hz, H-8''), 5.94 (1H, d, 2.2 Hz, H-6''), 5.80 (1H, d, 12.0 Hz, H-2''), 4.51 (1H, d, 12.0 Hz, H-3'')	7.71 (1H, dd, 8.6, 2.1 Hz, H-6'), 7.49 (1H, br s, 2.1 Hz, H-2'), 7.18 (2H, AA', H-2'''/H-6'''), 6.87 (1H, d, 8.6 Hz, H-5'), 6.66 (2H, XX', H-3'''/H-5'''), 6.62 (1H, d, 2.1 Hz, H-8), 6.50 (1H, s, H-3), 6.33 (1H, d, 2.1 Hz, H-6), 5.95 (2H, AB system, H-6'' and H-8''), 5.80 (1H, d, 11.8 Hz, H-2''), 4.53 (1H, d, 11.8 Hz, H-3''), 3.89 (3H, s, O-Me)

Peak	<u>4</u>	<u>5</u>	<u>6</u>
Name	Ochnaflavone	2'',3''-Dihydroochnaflavone	Ochnaflavone-7''-O-methyleter
Structure	<p>4: R=H 6: R=CH₃</p>		
RT (min)	42.19	45.10	63.85
<i>m/z</i> (MF, ppm)	539.0953 [M+H] ⁺ (C ₃₀ H ₁₉ O ₁₀ ⁺ , ΔM 3.8)	541.1102 [M+H] ⁺ (C ₃₀ H ₂₁ O ₁₀ ⁺ , ΔM 4.7)	553.1084 [M+H] ⁺ (C ₃₁ H ₂₁ O ₁₀ ⁺ , ΔM 7.0)
¹ H NMR ((nH, m, J (in Hz))	8.02 (2H, d, 8.7 Hz, H-2''''/H-6'''), 7.87 (1H, br d, 8.4 Hz, H-6'), 7.86 (1H, br s, H-2'), 7.14 (1H, d, 8.4 Hz, H-5'), 7.02 (2H, d, 8.7 Hz, H-3''''/H-5'''), 6.82 (1H, s, H-3 or H-3'), 6.82 (1H, s, , H-3 or H-3'), 6.47 (1H, d, 1.4 Hz, H-8 or H-8'), 6.46 (1H, d, 1.4 Hz, H-8 or H-8'), 6.18 (1H, d, 1.4 Hz, H-6 or H-6'), 6.17 (1H, d, 1.4 Hz, H-6 or H-6')	7.74 (1H, br d, 8.4 Hz, H-6'), 7.59 (1H, br s, H-2'), 7.49 (2H, d, 8.3 Hz, H-2''''/H-6'''), 7.11 (1H, d, 8.4 Hz, H-5'), 7.02 (2H, d, 8.3 Hz, H-3''''/H-5'''), 6.56 (1H, s, H-3), 6.40 (1H, br s, H-8), 6.20 (1H, br s, H-6), 5.93 (1H, br s, H-8''), 5.89 (1H, d, 1.5 Hz, H-6''), 5.44 (1H, dd, 12.9, 2.7 Hz, H-2''), 3.12 (1H, dd, 17.2, 12.9 Hz, H-3''A), 2.78 (1H, dd, 17.2, 2.7 Hz, H-3''B)	8.06 (2H, d, 8.6 Hz, H-2''''/6'''), 7.85 (1H, d, 8.1 Hz, H-6'), 7.84 (1H, s, H-2'), 7.10 (1H, d, 8.1 Hz, H-5'), 7.03 (2H, d, 8.6 Hz, H-3''''/H-5'''), 6.91 (1H, s, H-3''), 6.79 (1H, s, H-3), 6.76 (1H, br s, H-8''), 6.46 (1H, br s, H-8), 6.38 (1H, br s, H-6''), 6.16 (1H, br s, H-6) 3.87 (3H, s, O-Me)

Peak	<u>7</u>	<u>8</u>	<u>9</u>
Name	Isombamichalcone	Lophirone A	(1 β ,2 α)-di-(2,4-dihydroxybenzoyl)- (3 β ,4 α)-di-(4-hydroxyphenyl)- cyclobutane
Structure			
RT (min)	20.26	20.84	21.36
<i>m/z</i> (MF, ppm)	515.1725 [M+H] ⁺ (C ₃₀ H ₂₇ O ₈ ⁺ , ΔM 4.8)	511.1379 [M+H] ⁺ (C ₃₀ H ₂₃ O ₈ ⁺ , ΔM 2.1)	513.1520 [M+H] ⁺ (C ₃₀ H ₂₅ O ₈ ⁺ , ΔM 4.3)
¹ H NMR ((nH, m, J (in Hz))	7.38 (1H, d 8.3 Hz, H-6'''), 7.24 (2H, AA', H-2/H-6), 6.79 (2H, XX', H-3/H-5), 6.69 (2H, AA', H-2''/H-6''), 6.49 (2H, XX', H-3''/H-5''), 6.39 (1H, d, 8.8 Hz, H-6'), 6.39 (1H, dd, 8.3 Hz, J _{H-3''':H-5'''} impossible to measure due to peaks overlapping, H-5'''), 6.34 (1H, d, 2.5 Hz, H-3'), 6.11 (1H, d, 2.2 Hz, H-3'''), 5.85 (1H, dd, 8.8, 2.5 Hz, H-5'), 5.50 (1H, d, 6.6 Hz, H-C'), 5.09 (1H, d, 7.0 Hz, H-β), 3.75 (1H, dd, 7.0 Hz, 4.3 Hz, H-α), 3.22 (1H, m, H-α'), 2.37 (1H, dd, 13.9 Hz, 4.5 Hz, H-β'A), 2.14 (1H, t, 13.2 Hz, H-β'B)	8.23 (1H, s, H-1), 8.15 (1H, d, 9.0 Hz, H-17), 7.88 (1H, d, 8.9 Hz, H-5), 7.16 (2H, AA')*, 7.13 (2H, AA')*, 6.85 (1H, dd, 8.9 Hz, 1.9 Hz, H-6), 6.72 (1H, m, H-8), 6.59 (2H, XX')**, 6.55 (2H, XX')**, 6.34 (1H, dd, 9.0 Hz, 2.3 Hz, H-16), 6.14 (1H, dd, 2.3 Hz, 1.1 Hz, H-14), 6.00 (1H, d, 12.1 Hz, H-10), 4.67 (1H, d, 12.1 Hz, H-18) *impossible to assign (H-20/H-24, H-26/H-30) ** impossible to assign (H-21/H-23, H-27/H-29)	7.68 (2H, d, 8.8 Hz, H-6 A/A'), 6.90 (4H, AA', H-2/H-6 B/B'), 6.77 (4H, XX', H-3/H-5 B/B'), 6.49 (2H, dd, 8.8, 2.3 Hz, H-5 A/A'), 6.26 (2H, d, 2.3 Hz, H-3 A/A'), 5.85 (2H, d, 12.0 Hz, H-1/H-2 C), 2.66 (2H, d, 12.0 Hz, H-3/H-4 C)

Peak	10	11
Name	Lophirone F	Lophirone C
Structure		
RT (min)	22.05	26.49
<i>m/z</i> (ppm)	529.1499 [M+H] ⁺ (C ₃₀ H ₂₅ O ₉ ⁺ , ΔM 1.2)	511.1368 [M+H] ⁺ (C ₃₀ H ₂₃ O ₈ ⁺ , ΔM 4.1)
¹ H NMR ((nH, m, J (in Hz))	7.58 (1H, d, 9.0 Hz, H-6'''), 7.37 (2H, AA', H-2/H-6), 7.28 (1H, d, 9.0 Hz, H-6'), 7.12 (2H, AA', H-2''/H-6''), 6.79 (2H, XX', H-3/H-5), 6.55 (2H, XX', H-3''/H-5''), 6.25 (1H, dd, 9.0 Hz, 2.3 Hz, H-5'''), 6.19 (1H, d, 2.3 Hz, H-3'), 6.10 (1H, dd, 9.0 Hz, 2.3 Hz, H-5'), 6.03 (1H, d, 2.3 Hz, H-3'''), 5.55 (1H, d, 9.0 Hz, H-β'), 5.09 (1H, dd, 9.0, H-β), 4.98 (1H, dd, 9.0 Hz, 7.9 Hz H-α'), 4.84 (1H, m, H-α)	7.88 (1H, d, 8.8 Hz, H-6'), 7.77 (1H, dd, 8.9 Hz, 1.0 Hz, H-6), 7.75 (1H, d, 15.3 Hz, α), 7.70 (1H, d, 8.8 Hz, H-6''), 7.55 (1H, d, 15.3 Hz, β), 7.43 (1H, d, 1.0 Hz, H-2), 7.23 (2H, AA', H-2''/H-6''), 6.96 (1H, d, 8.5 Hz, H-5) 6.81 (2H, XX', H-3''/H-5''), 6.45 (1H, dd, 8.8 Hz, 2.4 Hz, H-5'''), 6.41 (1H, dd 8.9 Hz, 2.4 Hz, H-5'), 6.36 (1H, d, 2.4 Hz, H-3'''), 6.29 (1H, d, 2.4 Hz, H-3'), 6.11 (1H, d, 7.1 Hz, α'), 5.37 (1H, d, 7.1 Hz, β')

The skeleton of the compounds is numbered following the literature where they have been previously reported (66, 67, 69, 71-73, 100, 102).

4.6.1 Structure elucidation

DQF-COSY of compound **1** implied the presence of three discrete spin systems as shown in Figure 15. Two AA'XX' spin systems in the downfield region of ^1H NMR spectrum corresponded to two *para*-substituted benzenes. The third spin system (marked red) was formed by seven resonances with chemical shifts between 4.74 and 3.42 ppm which were attributed to glucose. Due to a poor HMBC spectrum it was impossible to study linkages between the three moieties. However, HRMS data and comparison of chemical shifts in the literature revealed compound **1** to be lanceoloside A. Lanceoloside A was previously isolated from the methanol extract of the leaves of *Lophira lanceolata* (73).

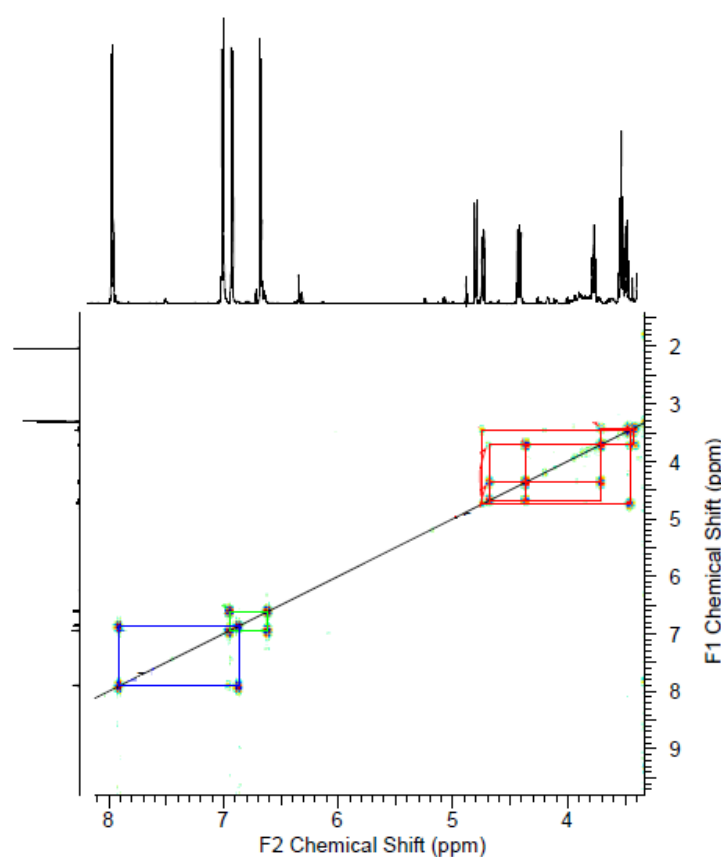


Figure 15: DQF-COSY spectrum of lanceoloside A (**1**) with three distinct spin systems marked with blue, green and red.

HRMS data of compound **2** showed a base peak at m/z 541.1114 which was attributed to $\text{C}_{30}\text{H}_{21}\text{O}_{10}^+$ and a base peak at m/z 555.1263 for compound **3** which suggested its molecular formula to be $\text{C}_{31}\text{H}_{22}\text{O}_{10}$. This implied that compound **3** could be a methylated version of compound **2** which was proven with the analysis of ^1H NMR spectra. Chemical shifts and multiplicity of the signals for all protons were comparable. The main difference between the

two spectra was the resonance at δ_{H} 3.89 ppm (3H) and shifted signals for H-6 and H-8 in the spectrum of **3** which suggested that the CH_3O - substituent is placed on C-7. (Figure 16) Comparison of ^1H NMR data we obtained with the data found in the literature (72) confirmed **2** to be lanceolatin A and **3** to be lanceolatin B. Both compounds were previously isolated from the methanol extract of the leaves of *Lophira lanceolata* (72).

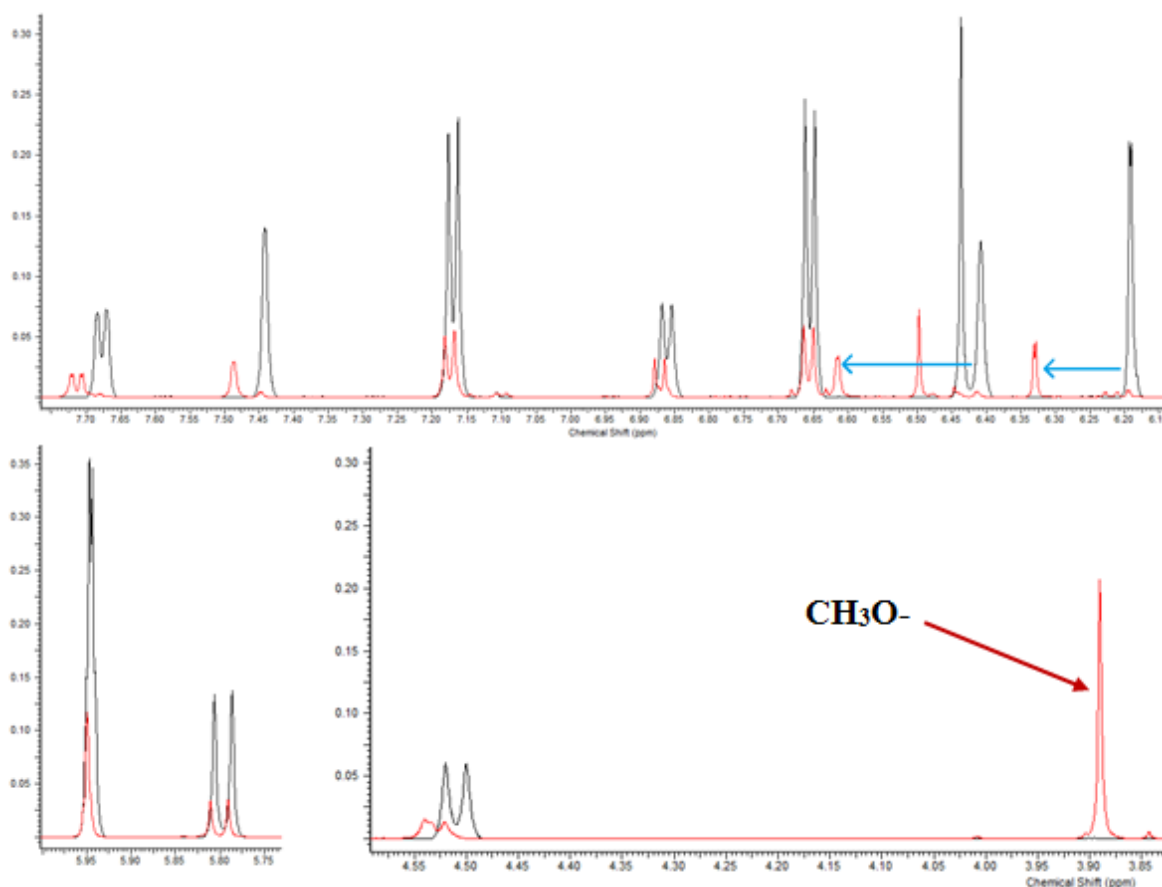


Figure 16: ^1H NMR spectrum of lanceolatin A (**2**) (black) overlaid by ^1H NMR spectrum of lanceolatin B (**3**) (red); the main difference is the singlet at δ_{H} 3.89 ppm (3H) in the spectrum of lanceolatin B (dark red arrow) and shifted peaks for H-6 and H-8 (blue arrows)

HRMS analysis revealed that molecular formulae for compounds **4**, **5** and **6** were $\text{C}_{30}\text{H}_{18}\text{O}_{10}$, $\text{C}_{30}\text{H}_{20}\text{O}_{10}$ and $\text{C}_{31}\text{H}_{20}\text{O}_{10}$, respectively, which suggested that there is a high probability that the compounds were structurally related to the active compound (**2**), lanceolatin A, and lanceolatin B (**3**). However, it was soon confirmed that compounds with above stated formulas have never been isolated neither from *Lophira lanceolata* nor from the genus *Lophira*.

^1H NMR spectrum of compound **4** showed two pairs of *meta*-coupled protons at δ_{H} 6.47 (1H, d, 1.4 Hz), δ_{H} 6.46 (1H, d, 1.4 Hz), δ_{H} 6.18 (1H, d, 1.4 Hz), δ_{H} 6.17 (1H, d, 1.4 Hz) and two

singlets at δ_{H} 6.82 ppm overlapping. Along the lines of lanceolatin A (**2**) and lanceolatin B (**3**) it was possible to conclude **4** comprises two 5,7-dihydroxychromone moieties. In addition, 1, 2, 4 – trisubstituted (δ_{H} 7.87, 1H, br d, 8.4 Hz; δ_{H} 7.86, 1H, br s; δ_{H} 7.14, 1H, d, 8.4 Hz) and *para*-substituted benzene ring protons were detected (δ_{H} 8.02, 2H, d, 8.7 Hz; δ_{H} 7.02, 2H, d, 8.7 Hz). With the support of the HRMS data we assumed compound **4** includes two apigenins linked at C-3' and 4'' and therefore, **4** was identified as ochnaflavone. Ochnaflavone was predominantly found in representatives of the *Ochna* genus and has been proposed as a taxonomic marker of the genus (100-106). However, it has been also isolated from plants of the *Godoya* (107) and *Cespedesia* (108) genera, (Ochnaceae) and from *Lonicera japonica* (Caprifoliaceae) (109).

Compared to ochnaflavone (**4**), the ^1H NMR spectrum of compound **5** displayed three additional resonances δ_{H} 5.44 (1H, dd, 12.9 Hz, 2.7 Hz), 3.12 (1H, dd, 17.2 Hz, 12.9 Hz), 2.78 (1H, dd, 17.2 Hz, 2.7 Hz). However, one of the H-3/3' flavone singlets seen in ^1H NMR spectrum of ochnaflavone (**4**) was absent, which together with HRMS data implied a reduction of a double bond in one of the 4-pyrone rings. The HMBC spectrum revealed a cross-peak between δ_{H} 7.49, which is part of the *para*-substituted benzene, and δ_{C} 79.6, which is separated by one bond with the hydrogen resonating at δ_{H} 5.44 ppm (Figure 17). In addition, it was possible to detect cross-correlations in the NOESY spectrum between hydrogens of the 1, 2, 4 – trisubstituted benzene (δ_{H} 7.74 and 7.59) and the remaining singlet belonging to the flavone moiety (δ_{H} 6.56) as well as cross-peaks between δ_{H} 7.49 \rightarrow δ_{H} 5.44 and δ_{H} 7.49 \rightarrow δ_{H} 3.12. Therefore we concluded that compound **5** has a single bond between 2'' and 3'' and identified it as 2'',3''- dihydroochnaflavone. The compound has previously been isolated from plants of the Ochnaceae family (102,107) but also from *Quintinia acutifolia* (Grossulariaceae) (109) and *Selaginella labordei* (Seleginellaceae) (111).

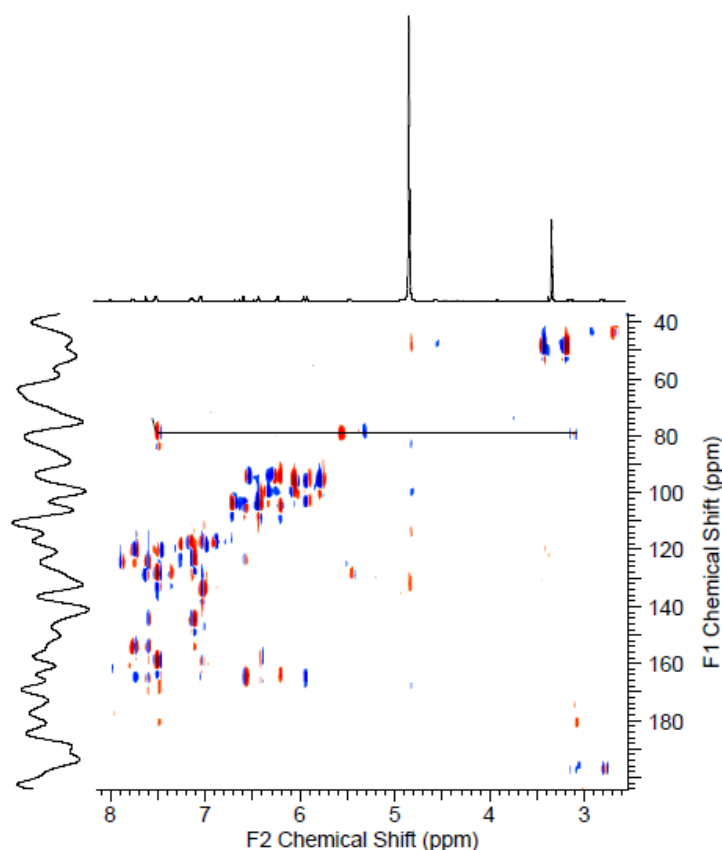


Figure 17: HMBC spectrum of 2'',3''-dihydroochnaflavone (**5**) showing cross-peaks between δ_{H} 7.49 (part of the *para*-substituted benzene) and δ_{H} 3.12 (H-3'') to δ_{C} 79.6 (C-2'') which is separated by one bond with the hydrogen resonating at δ_{H} 5.44 (H-2''). A ^{13}C spectrum was not recorded separately therefore the 2D spectrum shows a projection of it

The main difference between the ^1H NMR spectra of ochnaflavone (**4**) and compound **6** was the additional singlet seen at δ_{H} 3.87 ppm, integrated to three protons, found in the spectrum of **6**. That suggested that one of the hydroxyl groups was methylated which was confirmed by HRMS analysis. Moreover, the resonances of the protons members of one of the benzopyran-4-one rings were shifted to a higher chemical shift (δ_{H} 6.91, 6.76 and 6.38) if compared to ochnaflavone (**4**) which implied the CH_3O - substituent is placed on the benzopyran-4-one ring. To determine the position of the methoxy group NOESY and HMBC spectra were studied. NOESY showed cross-peaks between δ_{H} 6.91 and δ_{H} 8.06, being part of the *para*-substituted benzene, as well as δ_{H} 6.79, the singlet of the benzopyran-4-one that was not methylated and δ_{H} 7.84/7.85, both part of the three-substituted benzene (Figure 18). Therefore we concluded that the CH_3O - group could be positioned on C-5'' or C-7''. However, HMBC spectrum revealed a cross-peak between the methoxy group (δ_{H} 3.87) and

δ_C 165.7 as well as δ_H 6.76 (H-8'') and δ_C 165.7 which confirmed that the CH_3O - was positioned on C-7''. Therefore, **6** was identified as ochnaflavone 7''-O-methylether. Ochnaflavone 7''-O-methylether was previously isolated from *Ochna integerrima* (102), *Cespedesia spathulata* and *Cespedesia macrophylla* (108), all three belonging to the Ochnaceae family. To the best of our knowledge we are reporting the complete ^1H NMR data of **6** for the first time.

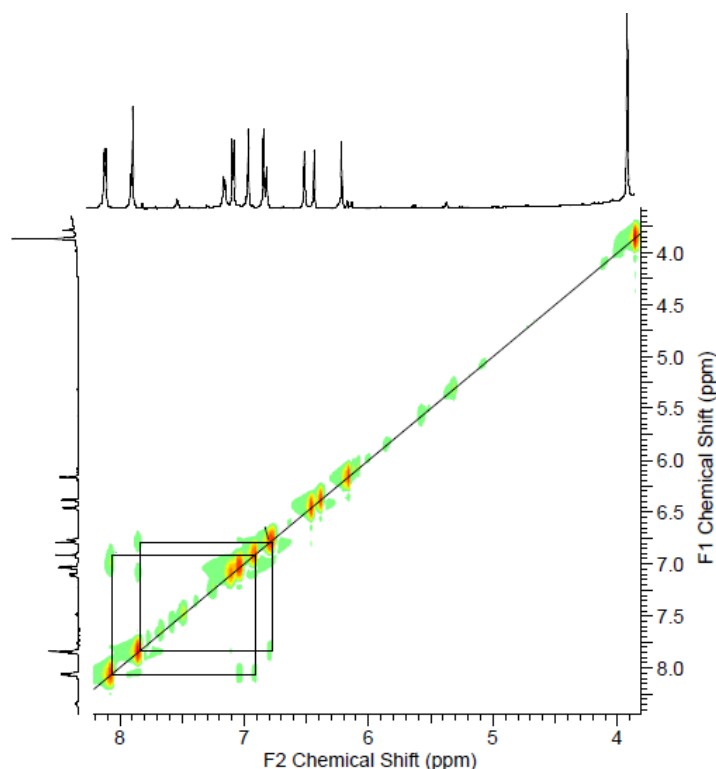


Figure 18: NOESY spectrum of ochnaflavone 7''-O-methylether (**6**) showing cross-peaks δ_H 6.91 - δ_H 8.06 and δ_H 6.79 - δ_H 7.84/7.85. The signal at δ_H 3.87 ppm does not display any correlations

^1H NMR spectra of compounds **7** and **10** showed similar features: two AA'XX' spin systems, two AMX spin systems, both in the aromatic region, and two relatively deshielded doublets. Furthermore, it was possible to observe four additional resonances for compound **7** (δ_H 3.75, 3.22, 2.37, 2.14 ppm) and two additional resonances for compound **10** (δ_H 4.98, 4.84 ppm). From the ^1H NMR data and HRMS data we assumed **7** is isombamichalcone which was previously isolated from the ethyl acetate extract of the stem bark of *Lophira lanceolata* (71). Whereas compound **10** was confirmed to be lophirone F and not its configurational isomer lophirone G. Both were previously isolated from the acetone extract of the stem bark of *Lophira lanceolata*. (69) Lophirone G is an axial symmetric compound and therefore its

^1H NMR spectrum would show half the number of signals as compared to those of lophirone F. The connections between the tetrahydrofuran ring and the aromatics were studied by HMBC. The relative stereochemistry of the tetrahydrofuran protons was confirmed by the NOE correlations observed in NOESY spectra between *cis* oriented protons and the absence of the correlations between *trans*-oriented protons (Figure 19). J couplings between *trans* protons are relatively small, however comparable to the ones listed in the literature (69, 71).

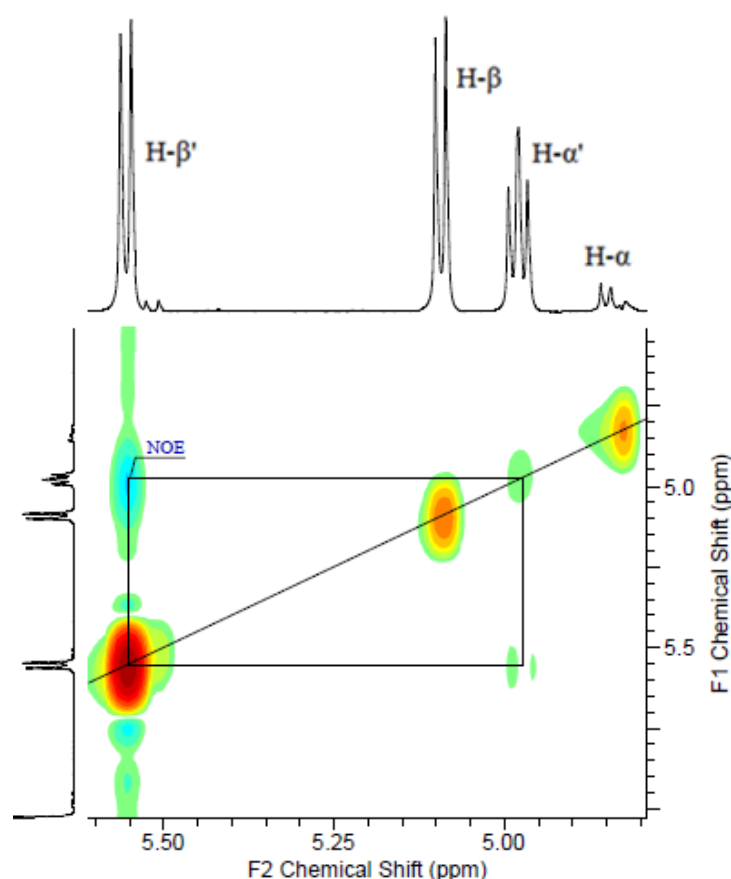


Figure 19: NOESY spectrum of lophirone F (**10**) showing NOE correlations between *cis* oriented protons

^1H NMR spectrum together with DQF-COSY data of compound **8** enabled the distinction of two 1, 4 – disubstituted (AA'XX') and two 1, 2, 4 – trisubstituted (AMX) aromatic rings, in addition to an AX system (δ_{H} 6.00 and 4.76 ppm, $J = 12.1$ Hz) and a singlet with a high chemical shift (δ_{H} 8.23). All of the above listed signals correspond to the structure of lophirone A which was previously isolated from the acetone extract of *Lophira lanceolata* stem bark (66). HRMS analysis confirmed its molecular formula (HR-ESIMS $^{+}$) m/z 511.1379 $[\text{M}+\text{H}]^{+}$ [$\text{C}_{30}\text{H}_{23}\text{O}_8^{+}$, ΔM 2.1 ppm). However, to verify the structure we studied the ^1H - ^{13}C heteronuclear multiple bond correlations (Figure 20). Long-range correlations

between the methine proton at δ_{H} 4.67 ppm and the carbons of 1,4-disubstituted benzenes confirmed the bonds between the methine group and the *para*-substituted aromatic rings. Furthermore, the resonance found at δ_{H} 6.00 shows correlation to δ_{C} 123.3 (C2), 156.9 (C1), 176.3 (C3) which form the heterocyclic ring, to δ_{C} 204.5 (carbonyl carbon C11) and to δ_{C} 134.1 (C17), being part of A' ring. In addition, the resonance at δ_{H} 8.15 (H17) correlated to the carbonyl carbon confirming the linkage with the A' ring-(C=O)-C10. On the other hand, it was possible to detect cross-peaks between the following resonances δ_{H} 7.88 (H5) \rightarrow δ_{C} 176.3 (C3), 163.8 (C7), 158.6 (C9); δ_{H} 6.85 (H6) \rightarrow δ_{C} 118.9 (C4), δ_{C} 102.9 (C8); δ_{H} 6.72 (H8) \rightarrow δ_{C} 118.9 (C4), 163.8 (C7), 158.6 (C9) and δ_{H} 8.23 (H1) \rightarrow δ_{C} 123.3 (C2), 176.3 (C3), 158.6 (C9) confirming the fusion of the AMX aromatic and 4-pyrone rings.

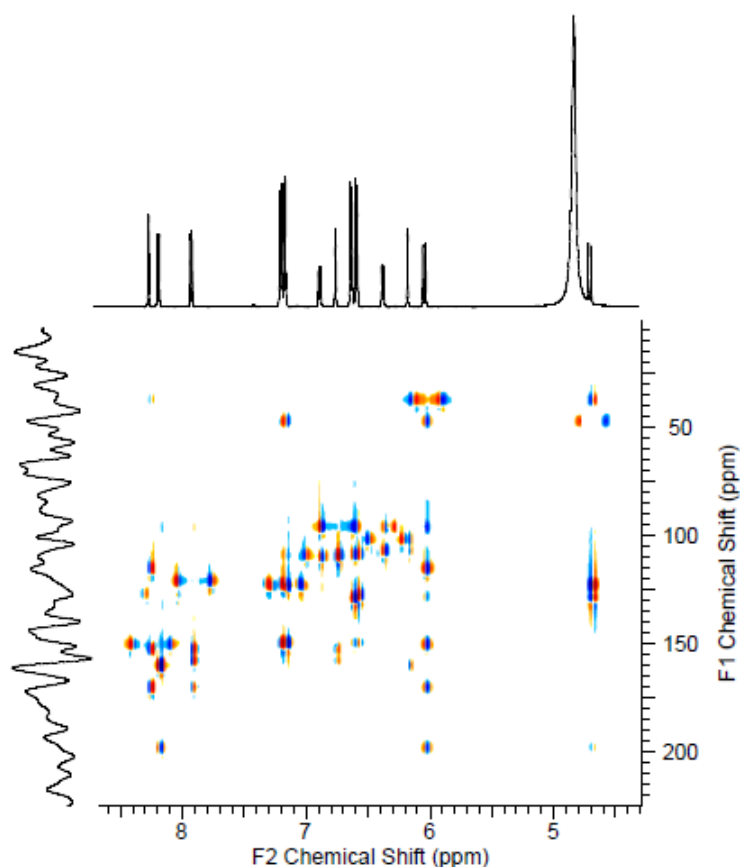


Figure 20: HMBC spectrum of lophirone A (**8**) showing correlations between carbons and protons separated by two, three and four bonds. A ^{13}C spectrum was not recorded separately therefore the 2D spectrum shows a projection of it

HRMS data of compound **9** showed a base peak at m/z 513.1520 $[\text{M}+\text{H}]^+$ which was attributed to $\text{C}_{30}\text{H}_{25}\text{O}_8^+$. ^1H NMR spectrum exhibited just seven distinct resonances,

indicating a symmetric molecule. The signals at δ_{H} 6.90 and 6.77 ppm were integrated to four protons each and their typical AA'XX' pattern suggested the presence of two *para*-substituted benzenes. The five remaining signals were all integrated to two nuclei. Protons resonating at δ_{H} 7.68, 6.49 and 6.26 are part of two 1, 2, 4-substituted benzenes. Each of the doublets (δ_{H} 5.85 and 2.66) represent two mutually coupled methine protons associated with a cyclobutyl moiety. Their *trans* configuration was confirmed by a large coupling constant (12.0 Hz) and the absence of cross-peaks in NOESY spectrum. Compound **9** was identified as (1 β ,2 α)-di-(2,4-dihydroxybenzoyl)-(3 β ,4 α)-di-(4-hydroxyphenyl)-cyclobutane after studying the linkage between the cyclobutan ring and the 4-hydroxyphenyls and the 2,4-dihydroxybenzoyls by HMBC and NOESY. The dimeric dihydrochalcone has never been found in *Lophira lanceolata* before. To the best of our knowledge, the compound has been previously isolated just once as a peracetate derivative from the roots of *Agapanthus africanus* (Liliaceae) (112).

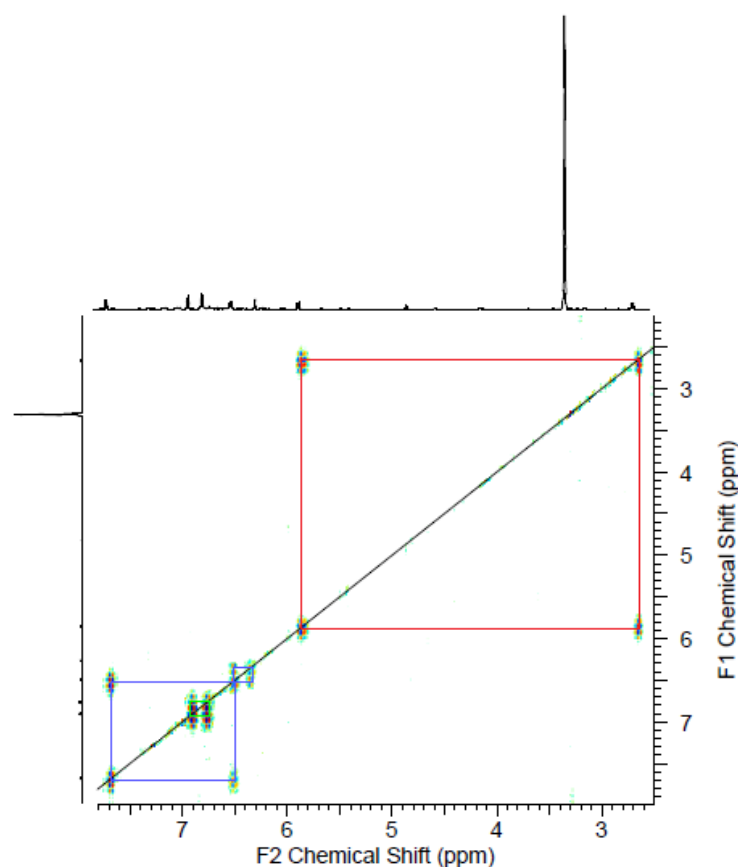


Figure 21: COSY spectrum of (1 β ,2 α)-di-(2,4-dihydroxybenzoyl)-(3 β ,4 α)-di-(4-hydroxyphenyl)-cyclobutane (**9**) showing three distinct spin system; a cyclobutan ring (red), a 1,2,4-trisubstituted benzene (blue) and 1,4-disubstituted benzene (green)

On the basis of HRMS data, compound **11** was assigned to the molecular formula $C_{30}H_{23}O_8$. In addition to lophirone A (**8**), there are two other compounds (lophirone B and lophirone C) that were previously isolated from the stem bark of *Lophira lanceolata* with the same molecular formula (67). 1H NMR and COSY spectra revealed one AA'XX' spin system in the aromatic region of the spectrum implying the presence of a *para*-substituted benzene, three AMX spin systems in the aromatic area suggesting three trisubstituted benzenes and four doublets in the downfield part of the spectrum. All these characteristics were found in lophirone C whose structure was confirmed after comparing the 1H NMR data we obtained with the data found in the literature (67).

4.7 Antifungal characterization

Based on the initial high-resolution PM H^+ -ATPase inhibition screening and the subsequent chemical profiling of the extracts of the leaves and the stem bark of *Lophira lanceolata*, we decided to subject lanceolatin A (**2**), lanceolatin B (**3**) and lophirone A (**8**) to a detailed antifungal characterization. IC_{50} values for fungal plasma membrane H^+ -ATPase inhibition together with MIC for 50 % inhibition of fungal growth of *Saccharomyces cerevisiae* and *Candida albicans* were assessed for each of the tested compounds. Additionally, we decided to determine the IC_{50} values for Na^+/K^+ ATPase. The results are shown in Table IX.

The inhibition of the fungal PM H^+ -ATPase is the first reported pharmacological activity for lanceolatin A, while lophirone A has previously been shown to exhibit tumour promotion inhibition through several mechanisms (113).

Table IX: IC_{50} values for PM H^+ -ATPase and Na^+/K^+ -ATPase together with MIC for 50 % inhibition of *S. cerevisiae* and *C. albicans*. The average IC_{50} of triplicates along with their respective standard deviations are given.

Compound	IC_{50}^a [μM]		MIC for 50 % inhibition [μM]	
	PM H^+ -ATPase	Na^+/K^+ -ATPase	<i>Saccharomyces cerevisiae</i>	<i>Candida albicans</i>
Lanceolatin A (2)	13.5 ± 0.3	3.0 ± 0.3	>150	>150
Lophirone A (8)	15.1 ± 0.4	40.9 ± 23.8	>150	>150
Orthovanadate	0.27 ± 0.02	-	-	-

^a $n=3$; ^b $n=2$

4.7.1 PM H⁺-ATPase inhibition and structure-activity relationship

We decided to determine the IC₅₀ against PM H⁺-ATPase for orthovanadate (Figure 22) as it is the only well-characterized inhibitor of the fungal proton pump so far (114).

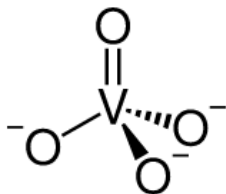


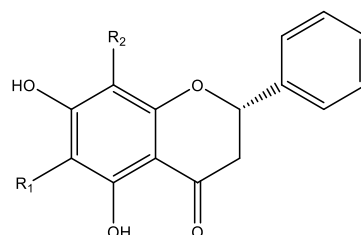
Figure 22: Orthovanadate

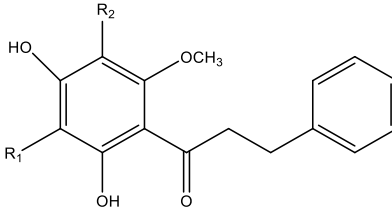
The antagonist potency of both lanceolatin A (**2**) and lophirone A (**8**) were significantly weaker in comparison to the potency of orthovanadate. Lanceolatin B (**3**) did not show activity in the soluble range in DMSO and it is therefore not reported in the table.

Ebselen, a synthetic organoselenium compound was also shown to have a stronger activity on the fungal proton pump (115). The inhibitory effects of lanceolatin A and lophirone A are comparable to the effects exhibited by the compounds previously isolated from a series of African plants and characterized by Staerk and co-workers (56, 57). The compounds with their respective IC₅₀ values are reported in the table X.

Table X: Compounds previously tested for their ability to inhibit PM H⁺-ATPase with their corresponding IC₅₀ values.

Compound	IC ₅₀ [μM]	Structure
Ebselen	3.0	synthetic organoselenium compound
Chebulagic acid	15.8 ± 7.9	tannin
Tellimagrandin II	10.6 ± 3.1	tannin
Pinocembrin	>333	R ₁ =R ₂ =H
Isochamanetin	66.6 ± 11.6	R ₁ =o-hydroxybenzyl R ₂ =H
Chamanetin	64.2 ± 6.0	R ₁ =H R ₂ = o-hydroxybenzyl
Dichamamentin	7.4 ± 0.8	R ₁ =R ₂ = o-hydroxybenzyl



Uvaretin	33.7 ± 5.7	$R_1 = o\text{-hydroxybenzyl}$ $R_2 = H$	
Diuvaretin	19.2 ± 3.7	$R_1 = R_2 = o\text{-hydroxybenzyl}$	

Chebulagic acid and tellimagrandin II both isolated from *Haplocoelum foliolosum* (56) are hydrolysable tannins and are structurally not related to lanceolatin A and lophirone A. Pinocembrin, isochamanetin, chamanetin, dichamanetin, uvaretin and diuvaretin found in *Uvaria Chamae* (57) are flavanones and dihydrochalcones. The active metabolites from *Lophira lanceolata* leaves and stem bark are structurally related to them. The main features in common are the flavanone skeleton observed in lanceolatin A and in pinocembrin, isochamanetin, chamanetin, dichamanetin along with the dihydrochalcone backbone seen in lophirone A, uvaretin and diuvaretin. Therefore, we deduced that these two structural characteristics are responsible for the activity exhibited by the compounds. However, the information was too limited to establish any structure-activity relationship. Hence, further studies on semisynthetic analogues should be conducted. Compounds isolated from *Uvaria Chamae* showed that the introduction of *o*-hydroxybenzyl substituents on C-6 and C-8 of the flavanone ring and dihydrochalcone backbone increased the potency of the enzyme inhibition. Along the lines, one of the steps to investigate new inhibitors of the fungal proton pump could be the synthesis of *o*-hydroxybenzylated derivatives lanceolatin A and lophirone A.

The only difference between lanceolatin A (**2**) and 2'',3''-dihydroochnaflavone (**5**) is the position of the linkage between the flavanone and flavone moieties. Therefore, it would be interesting to investigate also on the antifungal properties of 2'',3''-dihydroochnaflavone (**5**). The high-resolution bioassay displayed a correlation between the compound and the enzyme inhibition, however significantly weaker in comparison to lanceolatin A. Ochnaflavone (**4**) differs from 2'',3''-dihydroochnaflavone (**5**) in the double bond in the 2'',3'' position and thus does not possess a flavanone skeleton. In the high-resolution screening ochnaflavone (**4**) did not show any activity. This information supports the earlier suggested hypothesis that the flavanone fragment is responsible for the fungal PM H⁺-ATPase inhibition exhibited by lanceolatin A. Despite the fact that it has been shown that some fungal

species are susceptible to flavones (116), it seems as their action is not mediated via the inhibition of the fungal proton pump.

The main difference between the active metabolite lophirone A (**8**) and other dihydrochalcone compounds isolated from the stem bark of *Lophira lanceolata* is that the “dihydro” fragment of lophirone A is not part of a ring. However, the information we have is too limited to make any assumptions on structure-activity relationship of dihydrochalcones.

4.7.2 Fungal growth inhibition

Lanceolatin A and lophirone A did not show inhibitory effects on the growth of *S. cerevisiae* and *C. albicans* at concentrations lower than 150 μM . Considering the inhibitory activity of the compounds on the isolated fungal PM H^+ -ATPase and no effect on the growth of the selected fungal strains, we can conclude that the active metabolites isolated from *Lophira lanceolata* act from the cytoplasmic side of the membrane. To observe effects on fungal growth, such compounds would need to penetrate the fungal cell wall and membrane. No inhibitory effects on the fungal growth can be therefore attributed to poor permeability of the compounds. Moreover, fungal efflux pumps could have also pumped out the active metabolites which resulted in no inhibition of the growth of the selected fungal strains.

Nevertheless, further studies on semisynthetic analogues with improved physicochemical properties should be conducted. To date the structure of the target enzyme has not been reported which further hinders the investigation. Testing hit compounds from *Lophira lanceolata* on fungal strains responsible for other serious infections in humans would be advantageous.

A study on Cameroonian plants showed that *Candida albicans* is susceptible to *L. lanceolata* leaf methanolic extract. However, in the disc-diffusion assay the extract did not inhibit the growth of the chosen strain at concentrations lower than 1024 $\mu\text{g/mL}$ (92). A subsequent study used the broth dilution technique to show that the MIC of *L. lanceolata* aqueous leaf extract is 6.25 mg/mL for both *C. albicans* and *Aspergillus niger* (93). Assuming the aqueous extract contained the same proportion of lanceolatin A as our ethyl acetate extract (9 %), the calculated concentration of the active metabolite of around 1040 μM would be significantly higher compared to lanceolatin A concentrations that we used (150 μM). Nevertheless, the proportion of lanceolatin A extracted in water could be considerably different and therefore, we cannot assume that lanceolatin A was responsible for the growth

inhibition. The fungal growth inhibition could have been the result of the synergistic activity of compounds present in the extract mixture.

4.7.3 Comment on High-Resolution Inhibition Assays

The inhibitory effects on fungal PM H⁺-ATPase of lanceolatin A (**2**) are slightly stronger in comparison to lophirone A (**8**), which was anticipated by the high-resolution PM H⁺-ATPase inhibition assay. None of the metabolites that inhibited fungal PM H⁺-ATPase showed correlation with fungal growth inhibition, which was confirmed after the isolation and antifungal characterization of individual compounds. Therefore, we can conclude that despite the anomalies displayed by the biochromatograms, the performed screening was adequate.

4.7.4 Na⁺/K⁺-ATPase inhibition and antifungal selectivity

We decided to test the selected compounds for their ability to inhibit of Na⁺/K⁺ ATPase. Na⁺/K⁺ ATPase and the fungal proton pump are both member of P-type ATPases and perform the same function – the establishment of electrochemical gradient which is the source of energy for secondary transport in cells. Contrary to H⁺-ATPases which are present in fungi, plants and protists, Na⁺/K⁺-ATPases are specific for animals. The human Na⁺/K⁺-ATPase is the most closely related structure to the fungal proton pump (30). Comparison of IC₅₀ values of both P-type ATPases gives a rough estimation of the potential selective toxicity of tested compounds.

As shown in Table IX lanceolatin A exhibits a stronger inhibitory activity on Na⁺/K⁺-ATPase (IC₅₀=3.0 ± 0.3 μM) than on the fungal proton pump (IC₅₀=13.5 ± 0.3 μM) whereas lophirone A showed stronger inhibition on our antifungal target. However, the standard deviation of the determination of IC₅₀ for Na⁺/K⁺-ATPase was high and therefore, the real IC₅₀ could be very similar to the IC₅₀ for the fungal proton pump. At this stage, the active metabolites from *L. lanceolata* seem not to possess the appropriate selective toxicity. Further studies on semisynthetic analogous with optimized structures should be conducted.

4.7.5 Flavanones and dihydrochalcones as antifungals

It has been previously shown that flavanones inhibit the growth of several fungal strains (116). However, the mechanism of their action has not been established yet. Several prenylated (117), halogenated (118), methoxylated (117-119), acetoxylated (120),

hydrazone, isoniazide (121), triazole (122) and imidazole (123) derivatives successfully inhibited fungal growth. Similarly, synthetic and semisynthetic analogues of lanceolatin A should be prepared and their potency against the fungal proton pump should be determined. Chemical modifications of our hit compounds could improve their poor effect on the growth of the tested fungal strains. As it was suggested the flavanone compounds applied together with existing azole antifungals could also improve the sensitivity of azole-resistant fungal strains (124).

To the best of our knowledge, dihydrochalcones have not been previously linked to antifungal activity. Uvaretin has been shown as the only dihydrochalcone to inhibit the growth of *S. cerevisiae* (57). Some natural occurring dihydrochalcones along with semisynthetic analogues have been tested for their ability to inhibit the growth of various fungi. None of them showed any activity (125, 126) which is consistent with our findings - lophirone A inhibited the fungal plasma membrane proton pump, however did not show any effect on the growth of *S. cerevisiae* and *C. albicans*.

5 CONCLUSION

The bioanalytical platform which combines high-resolution fungal plasma membrane H⁺-ATPase inhibition assay and high-performance liquid chromatography, high-resolution mass spectrometry, solid-phase extraction and nuclear magnetic resonance (HPLC-HRMS-SPE-NMR) supported the identification of two potential antifungal agents from the leaves and stem bark of *Lophira lanceolata*.

Defatted ethyl acetate extracts were tested for their ability to inhibit PM H⁺-ATPase as part of a larger screening project investigating the antifungal potential of African medicinal plants. Both leaf and stem bark crude extracts successfully inhibited fungal proton pump and showed a concentration-dependent activity profile.

The high-resolution PM H⁺-ATPase inhibition testing suggested that peak **2** from the leaf extract and peak **8** from the stem bark extract were responsible for the pharmacological activity exhibited by the crude extracts. Disappointingly, none of the peaks correlated with growth inhibition of *C. albicans* and *S. cerevisiae*. Due to the anomalies displayed by the biochromatograms, the reliability and the adequacy of the performed tests were questioned. However, a detailed antifungal characterization carried out afterwards confirmed the results of the high-resolution screening.

HPLC-HRMS-SPE-NMR proved to be a successful method for fast and efficient chemical analysis of major metabolites of *Lophira lanceolata* leaf and stem bark extracts. The only issue we encountered has been poor solubility of compounds **4** and **6** in the selected NMR solvent resulting in low S/N ratios in the NMR spectra. The coupled method does not favour the monitoring of the performance of each step and thus, it was impossible to observe the insolubility issue before the preparative scale isolation of the metabolites.

After a detailed HRMS, ¹H NMR and 2D NMR (DQF-COSY, NOESY, HSQC and HMBC) analysis **1** was identified as lanceoloside A, **2** as lanceolatin A, **3** as lanceolatin B, **4** as ochnaflavone, **5** as 2'',3''-dihydroochnaflavone, **6** as ochnaflavone-7''-O-methyleter, **7** as isombamichalcone, **8** as lophirone A, **9** as (1β,2α)-di-(2,4-dihydroxybenzoyl)-(3β,4α)-di-(4-hydroxyphenyl)-cyclobutane, **10** as lophirone F and **11** as lophirone C. **1-3**, **7**, **8**, **10**, **11** were previously found in *Lophira lanceolata* whereas for **4-6** and **9** this is the first reported isolation from the plant.

Preparative-scale isolation of active metabolites allowed determination of IC₅₀ values for PM H⁺-ATPase inhibition, IC₅₀ values for Na⁺/K⁺ ATPase inhibition and MIC for 50 % inhibition of fungal growth of *S. cerevisiae* and *C. albicans*. Lanceolatin A and lophirone A

exhibited a potent inhibition of the target with IC_{50} 13.5 and 15.1 μ M, respectively. However, they did not show any activity against fungal growth and did not exhibit appropriate selectivity. For both active metabolites this is the first report of their potential antifungal activity. Inhibitors of the fungal proton pump possessing a similar skeleton have been previously identified.

This study provides the basis for further development of novel inhibitors of the fungal PM H^+ -ATPase with flavanone and dihydrochalcone skeleton. The binding mode of the hit compounds should be determined and more potent semisynthetic and synthetic analogues should be prepared on that basis. Furthermore, co-crystallisation of the enzyme with the most potent inhibitors would allow the determination of key interactions between the compound and the amino acid residues in the enzyme active site. In the drug design process physicochemical properties should be taken in consideration in order to maximize fungal cell membrane permeability of the compounds. Additionally, further studies on the selective toxicity should be conducted.

6 REFERENCES

- 1) Cavalier-Smith T, A revised six - kingdom system of life, *Biological Reviews of the Cambridge Philosophical Society*, vol. 73, 1998, 203-266.
- 2) Cavalier-Smith T, Kingdoms Protozoa and Chromista and the eozoan root of the eukaryotic tree, *Biology Letters*, vol. 6, 2009, 342-345.
- 3) Encyclopaedia Britannica, <http://www.britannica.com/>, (Accessed 2.11.2015).
- 4) Huang B, Guo J, Yi B, Yu X, Sun L, Chen W, Heterologous production of secondary metabolites as pharmaceuticals in *Saccharomyces cerevisiae*, *Biotechnology Letters*, vol. 30, 2008, 1121-1137.
- 5) Brakhage AA, Spröte P, Al-Abdallah Q, Gehrke A, Plattner H, Tüncher A, Regulation of penicillin biosynthesis in filamentous fungi, *Advances in Biochemical Engineering/Biotechnology*, vol. 88, 2004, 45–90.
- 6) Deshpande MV, Mycopesticide production by fermentation: potential and challenges, *Critical Reviews in Microbiology*, vol. 25, 1999, 229–243.
- 7) Wasser Solomon P, Medicinal mushroom science: Current perspectives, advances, evidences, and challenges, *Biomedical Journal*, vol. 37, 2014, 345-356.
- 8) Pitt J. I., Hocking A. D., *Fungi and food spoilage*, third edition, Springer Science+Business Media LLC, Philadelphia, PA, 2009.
- 9) Oliveira M. P, Zannini E, Arendt E. K, Cereal fungal infection, mycotoxins, and lactic acid bacteria mediated bioprotection: From crop farming to cereal products, *Food Microbiology*, vol. 37, 2014, 78-95.
- 10) Oliveira P. M, Zannini E, Arendt E. K, Cereal fungal infection, mycotoxins, and lactic acid bacteria mediated bioprotection: From crop farming to cereal products, *Food Microbiology*, vol. 37, 2014, 78-95.
- 11) Peraica M, Radić M, Lucić A, Pavlović M, Toxic effects of mycotoxins in humans, *Bulletin of the World Health Organization*, vol. 77, 1999, 754-766.
- 12) Zain M. E, Impact of mycotoxins on humans and animals, *Journal of Saudi Chemical Society*, vol.15, 2011, 129–144.
- 13) Brown G. D, Denning D. W, Levitz S. M, Tackling human fungal infections, *Science*, vol. 336, 2012, 647.
- 14) Fungal Research Trust. How Common are Fungal Diseases? Updated 10/8/2011. Available on:

- <http://www.fungalresearchtrust.org/HowCommonareFungalDiseases2.pdf> (Accessed on 8.11.2015).
- 15) Kelly P. B, Superficial Fungal Infections, *Pediatrics in Review*, vol. 33, 2012, 22-37.
- 16) Puebla L. E. J, Fungal Infections in Immunosuppressed Patients, *Immunodeficiency*, 2012, Metodiev K. (Ed.), Available on <http://www.intechopen.com/books/immunodeficiency/fungal-infections-in-immunosuppressed-patients> (Accessed 10.11.2015).
- 17) McNeill M. M, Nash S. L, Hajjeh R. A, Phelan M. A, Conn L. A, Plikaytis B. D, Warnock D. W, Trends in mortality due to invasive mycotic diseases in the United States 1980-1997, *Clinical infectious diseases*, vol. 33, 2001, 641-647.
- 18) Richardson M. D, Warnock D. W, *Fungal Infection: Diagnosis and Management*, Fourth Edition, John Wiley & Sons, 2012, 5.
- 19) Kauffman C. A, Overview of Candida infections. In: UpToDate, Post TW (Ed), UpToDate, Waltham, MA, (Accessed on 3.2.2016).
- 20) Revankar S. G, Sobel J. D, Overview of fungal infections. In: Merck Manual Professional Edition. Available on: <http://www.merckmanuals.com/professional/infectious-diseases/fungi/overview-of-fungal-infections>, (Accessed on 3.2.2016).
- 21) Gubbins P. O, Anaissie E. J, Antifungal therapy. In: Anaissie E. J, McGinnis M. R, Pfaller M. A, *Clinical Mycology*, 2nd edition, Churchill Livingstone, Philadelphia, 2009, 161-195.
- 22) Vandeputte P, Ferrari S, Coste A. T, Antifungal Resistance and New Strategies to Control Fungal Infections, *International Journal of Microbiology*, vol. 2012, 2012, 26.
- 23) Odds F. C, Brown A. J. P, Gow N. A. R, Antifungal agents: Mechanism of action, *Trends in Microbiology*, vol. 11, 2003, 272-279.
- 24) Nucci M, Marr K. A, Emerging Fungal Diseases, *Clinical Infectious Diseases*, vol. 41, 2005, 521-526.
- 25) Serrano R, Structure and function of proton translocating ATPase in plasma membranes of plants and fungi, *Biochimica et Biophysica Acta*, vol. 947, 1988, 1-28.
- 26) Perlin D. S, Haber J. E, Genetic approaches to structure-function analysis in the yeast plasma membrane H⁺-ATPase, *Advances in Molecular and Cell Biology*, vol. 23, 1998, 143-166.

- 27) Monk B. C, Perlin D. S, Fungal plasma membrane proton pumps as promising new antifungal agents, *Critical Review in Microbiology*, vol. 20, 1994, 209-223.
- 28) Serrano R, Kielland-Brandt M. C, Fink G. R, Yeast Plasma membrane ATPase is essential for growth and has homolgy with (Na⁺ + K⁺), K⁺-and Ca²⁺-ATPases, *Nature*, vol. 319, 1986, 689-693.
- 29) Monk B.C, Mason A.B, Abramochkin G., Haber. J.E, Seto-Young D., Perlin D. S, The yeast plasma membrane proton pumping ATPase is a viable antifungal target. I. Effects of the cysteine-modifying reagent omeprazole, *Biochimica et Biophysica Acta*, vol. 1239, 1995, 81-90.
- 30) Seto-Young D, Monk B, Mason A. B, Perlin D. S, Exploring an antifungal target in the plasma membrane H⁺-ATPase of fungi, *Biochimica et Biophysica Acta (BBA) – Biomembranes*, vol. 1326, 1997, 249-256.
- 31) Dias D. A, Urban S, Roessner U, A historical overview of natural products in drug discovery, *Metabolites*, vol. 2, 2012, 303-336.
- 32) Chin Y, Kinghorn, A. D, Natural Products. In Manfred Schwab (Ed.): *Encyclopedia of Cancer*, Third edition, Springer Berlin Heidelberg, Heidelberg, 2012, 2465–2467.
- 33) McChesney J. D, Venkataraman S. K, Henri J. T, Plant natural products: Back to the future or into extinction?, *Phytochemistry*, vol. 68, 2007, 2015–2022.
- 34) Molinari G, Natural products in drug discovery: present status and prespectives, *Advances in experimental medicine and biology*, vol. 655, 2009, 13-27.
- 35) Boldi A. M, Libraries from natural products-like scaffolds, *Current Opinion in Chemical Biology* vol. 8, 2004, 281–286.
- 36) Rollinger J. M, Stuppner H, Langer T, Virtual screening for the discovery of the bioactive natural products, *Progress in Drug Research*, vol. 65, 2008, 213-249.
- 37) Baker D. D, Chu M, Oza U, Rajgarhia V, The value of natural products to future pharmaceutical discovery, *Natural Products Reports*, vol. 24, 2007, 1225-1244.
- 38) Ostrosky-Zeichner L, Casadevall A, Galgiani J. N, Odds F. C, Rex J. H, An insight into the antifungal pipeline: Selected new molecules and beyond, *Nature Review Drug Discovery*, vol. 9, 2010, 719–727.
- 39) Wink M, Plant breeding: importance of plant secondary metabolites for protection against pathogens and herbivores, *Theoretical and Applied Genetics*, vol. 75, 1988, 225-233.

- 40) Bennet R. N, Wallsgrove R. M, Secondary metabolites in plant defence mechanisms, *New Phytologist*, vol. 127, 1994, 617-633.
- 41) Cragg G. M, Newman D. J, Biodiversity: A continuing source of novel drug leads, *Pure and Applied Chemistry*, vol. 77, 2005, 7-24.
- 42) Negri M, Salci T. P, Shinobu-Mesquita C. S, Capoci I. R. G, Svidzinski T. I. E, Kioshima E. S, Early state research on antifungal natural products, *Molecules*, vol. 19, 2014, 2925-2956.
- 43) Dias D. A, Urban S, Roessner U, A Historical Overview of Natural Products in Drug Discovery, *Metabolites*, vol. 2, 2012, 303–336
- 44) Tu Y, Jeffries C, Ruas H, Nelson C, Smithson D, Shelat A. A, Brown K. M, Li X.-C, Hester J. P, Smillie T, Khan I. A, Walker L, Guy K, Yan B, An Automated High-Throughput System to Fractionate Plant Natural Products for Drug Discovery, *Journal of Natural Products*, vol. 73, 2010, 751-754.
- 45) Kongstad K. T, Özdemir C, Barzak A, Wubshet S. G, Staerk D, Combined use of high-resolution α -glucosidase inhibition profiling and HPLC-HRMS-SPE-NMR for investigation of antidiabetic principles in crude plant extracts, *Journal of Agricultural and Food Chemistry*, vol. 63, 2015, 2257-2263.
- 46) Liu B, Kongstad K. T, Qinglei S, Nyberg N, Jäger A, Staerk D, Dual high-resolution α -glucosidase and radical scavenging profiling combined with HPLC-HRMS-SPE-NMR for identification of minor and major constituents directly from the crude extract of *Pueraria lobata*, *Journal of Natural Products*, vol. 78, 2015, 294-300.
- 47) Wubshet S. G, Schmidt J. S, Wiese S, Staerk D, High-resolution screening combined with HPLC-HRMS-SPE-NMR for identification of potential health-promoting constituents in sea aster and searocket – New Nordic food ingredients, *Journal of Agricultural and Food Chemistry*, vol. 61, 2013, 8616-8623.
- 48) Schmidt J. S, Nyberg N. T, Staerk D, Assessment of constituents in *Allium* by multivariate data analysis, high-resolution α -glucosidase inhibition assay and HPLC-SPE-NMR, *Food Chemistry*, vol. 161, 2014, 192-198.
- 49) Wubshet S. G, Moresco H. H, Tahtah Y, Brighente I. M. C, Staerk D, High-resolution bioactivity profiling combined with HPLC-HRMS-SPE-NMR: α -glucosidase inhibitors and acetylated ellagic acid rhamnosides from *Myrcia palustris* DC. (Myrtaceae), *Phytochemistry*, vol. 116, 2015, 246-252.

- 50) Tahtah J, Kongstad K. T, Wubshet S. G, Nyber N, Jönsson L. H, Jäger A. K, Qinglei S, Staerk D, Triple aldose reductase/ α -glucosidase/radical scavenging high-resolution profiling combined with high-performance liquid chromatography – high-resolution mass spectrometry – solid-phase extraction – nuclear magnetic resonance spectroscopy for identification of antidiabetic constituents in crude extract of *Radix Scutellariae*, *Journal of Chromatography A*, vol. 1408, 2015, 125–132.
- 51) Okutan L, Kongstad K. T, Jäger A. K, Staerk D, High-resolution α -amylase assay combined with high-performance liquid chromatography – solid-phase extraction – nuclear magnetic resonance spectroscopy for expedited identification of α -amylase inhibitors — proof of concept and α -amylase inhibitor in cinnamon, *Journal of Agricultural and Food Chemistry*, vol. 62, 2014, 11465-11471.
- 52) Wubshet S. G, Nyberg N. T, Tejesvi M. V, Pirttilä A. M, Kajula M, Mattila S, Staerk D, Targeting high-performance liquid chromatography–high-resolution mass spectrometry–solid-phase extraction–nuclear magnetic resonance analysis with high-resolution radical scavenging profiles — bioactive secondary metabolites from the endophytic fungus *Penicillium namyslowskii*, *Journal of Chromatography A*, vol. 1302, 2013, 34-39.
- 53) Wiese S, Wubshet S. G, Nielsen J, Staerk D, Coupling HPLC–SPE–NMR with a microplate-based high-resolution antioxidant assay for efficient analysis of antioxidants in food — Validation and proof-of-concept study with caper buds, *Food Chemistry*, vol. 141, 2013, 4010-4018.
- 54) Liu Y, Staerk D, Nielsen M. N, Nyberg N, Jäger A. K, High-resolution hyaluronidase inhibition profiling combined with HPLC–HRMS–SPE–NMR for identification of anti-necrosis constituents in Chinese plants used to treat snakebite, *Phytochemistry*, vol. 119, 2015, 62-69.
- 55) Grosso C, Jäger A. K, Staerk D, Coupling of a high-resolution monoamine oxidase-A inhibitor assay and HPLC–SPE–NMR for advanced bioactivity-profiling of plant extracts, *Phytochemical Analysis*, vol. 24, 2013, 141-147.
- 56) Kongstad K. T, Wubshet S. G, Johannesen A, Kjellerup L, Winther A.-M. L, Jäger A. K, Staerk D, High-resolution screening combined with HPLC–HRMS–SPE–NMR for identification of fungal plasma membrane H⁺-ATPase inhibitors from plants, *Journal of Agricultural and Food Chemistry*, vol. 62, 2014, 5595-5602.

- 57) Kongstad K. T, Wubshet S. G, Kjellerup L, Winther A.-M. L, Staerk D, Fungal plasma membrane H⁺-ATPase inhibitory activity of o-hydroxybenzylated flavanones and chalcones from *Uvaria chamae* P. Beauv., *Fitoterapia*, vol. 105, 2015, 102-106.
- 58) Johansen K. T, Wubshet S. G, Nyberg N. T, Jaroszewski J. W, From retrospective assessment to prospective decisions in natural products isolation: HPLC-SPE-NMR analysis of *Carthamus oxyacantha*, *Journal of Natural Products*, vol. 74, 2011, 2454-2461.
- 59) Staerk D, Lambert M, Jaroszewski J. W, HPLC-NMR techniques for plant extract analysis, *Medicinal Plant Biotechnology. From Basic Research to Applications*, ed. Kayser O, Quax W, Wiley-VCH, Weinheim, 2006, 29-48.
- 60) Staerk D, Kesting J. R, Sairafianpour M, Witt M, Asili J, Emami S. A, Jaroszewski J. W, Accelerated dereplication of crude extracts using HPLC-PDA-MS-SPE-NMR: quinolinone alkaloids of *Haplophyllum acutifolium*, *Phytochemistry*, vol. 70, 2009, 1055-1061.
- 61) Sprogøe K, Staerk D, Ziegler H. L, Jensen T. H, Holm-Møller S. B, Jaroszewski J. W, Combining HPLC-PDA-MS-SPE-NMR with circular dichroism for complete natural product characterization in crude extracts: levorotatory gossypol in *Thespesia danis*, *Journal of Natural Products*, vol. 71, 2008, 516-519.
- 62) Hassler M, World Plants: Synonymic Checklists of the Vascular Plants of the World (version Jan 2015), In: *Species 2000 & IT IS Catalogue of Life, 2015 Annual Checklist* (Roskov Y, Abucay L, Orrell T, Nicolson D, Kunze T, Flann C, Bailly N, Kirk P, Bourgoin T, DeWalt R. E, Decock W, De Wever A, eds). Digital resource at www.catalogueoflife.org/col. Species 2000: Naturalis, Leiden, the Netherlands. ISSN 2405-8858.
- 63) Mapongmetsem P.-M, *Lophira lanceolata*, 2007. In: van der Vossen H. A. M, Mkamilo G. S, *Plant Resources of Tropical Africa 14. Vegetable oils*, PROTA Foundation, Wageningen, Netherlands/ Backhuys Publishers, Leiden, Netherlands/ CTA, Wageningen, Netherlands. 237 pp, 115-118.
- 64) Lohlum S. A, Maikidi G. H, Solomon M, Proximate composition, amino acid profile and phytochemical screening of *Lophira lanceolata* seeds, *African Journal of Food, Agriculture, Nutrition and Development*, vol. 10, 2010, 2012-2023.
- 65) Nonviho G, Paris C, Muniglia L, Sessou P, Agbangnan D. C. P, Brosse N, Sohounhloué D, Chemical characterization of *Lophira lanceolata* and *Carapa procera*

- seed oils: Analysis of Fatty Acids, Sterols, Tocopherols and Tocotrienols, *Research Journal of Chemical Sciences*, vol. 4, 2014, 57-62.
- 66) Ghogomu Tih R, Sondengam B. L, Martin M. T, Bodo B, Lophirone A, a biflavonoid with unusual skeleton from *Lophira lanceolata*, *Tetrahedron Letters*, vol. 28, 1987, 2967-2968.
- 67) Ghogomu Tih R, Sondengam B. L, Martin M. T, Bodo B, Structure of lophirones B and C, biflavonoids from the bark of *Lophira lanceolata*, *Phytochemistry*, vol. 28, 1989, 1557-1559.
- 68) Ghogomu Tih R, Sondengam B. L, Lophirones D and E: two new cleaved biflavonoids from *Lophira lanceolata*, *Journal of Natural Products*, vol. 52, 1989, 284-288.
- 69) Ghogomu Tih R, Sondengam B. L, Martin M. T, Bodo B, Structure of the chalcone dimers lophirone F, G and H from *Lophira lanceolata* stem bark, *Phytochemistry*, vol. 29, 1990, 2289-2293.
- 70) Ghogomu Tih R, Ewola Tih A, Sondengam B. L, Structures of lophirones I and J, minor cleaved chalcone dimers of *Lophira lanceolata*, *Journal of Natural Products*, vol. 57, 1994, 142-145.
- 71) Ghogomu Tih R, Sondengam B. L, Martin M. T, Bodo B, Structures of isombamichalcone and lophirochalcone, bi- and tetra-flavonoids from *Lophira lanceolata*, *Tetrahedron Letters*, vol. 30, 1989, 1807-1810.
- 72) Pegnyemb D. E, Ghogomu Tih R, Sondengam B. L, Minor biflavonoids of *Lophira lanceolata*, *Journal of Natural Products*, vol. 57, 1994, 1275-1278.
- 73) Pegnyemb D. E, Messanga B. B, Ghogomu R, Sondengam B. L, Martin M. T, Bodo B, A new benzoylglucoside and a new prenylated isoflavone from *Lophira lanceolata*, *Journal of Natural Products*, vol. 61, 1998, 801-803.
- 74) Sani A. A, Alemika T. E, Abdulraheem O. R, Sule I. M, Ilyas M, Haruna A. K, Sikirat A. S, Isolation and characterization of cupressuflavone from the leaves of *Lophira lanceolata*, *Journal of Pharmacy and Bioresources*, vol. 7, 2010.
- 75) Ali S. A, Abdulraheem R. O, Abdulkareem S. S, Alemika E. T, Ilyas M, Structure determination of betulinic acid from the leaves of *Lophira lanceolata* Van Tiegh. Ex Keay (Ochnaceae), *Journal of Applied Pharmaceutical Science*, vol. 1, 2011, 244-245.
- 76) Pegnyemb D. E, Messanga B. B, Ghogomu R. T, Sondengam B. L, Flavonoids from *Lophira lanceolata* leaves, *Fitoterapia*, vol. 69, 1998, 551.

- 77) Ali S. A, Ilyas M, Haruna A. K, Phytochemical screening of the leaves of *Lophira lanceolata* (Ochnaceae), Life Science Journal, vol. 4, 2007, 75-79.
- 78) Ewola Tih A, Ghogomu Tih R, Sondengam B. L, Martin M. T, Bodo B, Bongosin: a new chalcone-dimer from *Lophira alata*, Journal of Natural Products, vol. 53, 1990, 964-967.
- 79) Murakami A, Tanaka S, Ohigashi H, Hirota M, Irie R, Takeda N, Tatematsu A, Koshimizu K, Possible antitumor promoters: bi- and tetraflavonoids from *Lophira alata*, Phytochemistry, vol. 31, 1992, 2689-2693.
- 80) Pegnyemb D. E, Tih R. G, Sondengam B. L, Blond A, Bodo B, Biflavonoids from *Ochna afzelii*, Phytochemistry, vol. 57, 2001, 579-582.
- 81) Kaewamatawong R, Likhitwitayawuid K, Ruangrunsi N, Takayama H, Kitajima M, Aimi N, Novel biflavonoids from the stem bark of *Ochna integerrima*, Journal of Natural Products, vol. 65, 2002, 1027-1029.
- 82) Mbing J. N, Bassomo M. Y, Pegnyemb D. E, Tih R. G, Sondengam B. L, Blond A, Bodo B, Constituents of *Ouratea flava*, Biochemical Systematics and Ecology, vol. 31, 2003, 215-217.
- 83) Anuradha V, Srinivas Pullela V, Rao R. Ranga, Manjulatha K, Purohit Muralidhar G, Rao, J. Madhusudana, Isolation and synthesis of analgesic and anti-inflammatory compounds from *Ochna squarrosa* L., Bioorganic & Medicinal Chemistry, vol. 14, 2006, 6820-6826.
- 84) Tih A, Ghogomu Tih R, Sondengam B. L, Martin M. T, Bodo B, Tetraflavonoids of *Lophira alata*, Phytochemistry, vol. 31, 1992, 981-984.
- 85) Mbing J. N, Ndongo J. T, Enguehard-Gueiffier C, Atchade A, Pieboji J. G, Tih R. G, Pothier J, Pegnyemb D. E, Gueiffier A, Flavonoids from the leaves of *Ouratea zenkeri* and *Ouratea turnerae*, Asian Chemistry Letters, vol. 13, 2009, 81-88.
- 86) Tsukida K, Saiki K, Ito M, New isoflavone glycosides from *Iris florentina*, Phytochemistry, vol. 12, 1973, 2318-2319.
- 87) Bae K. H, Lee S. M, Lee E. S, Lee J. S, Kang J. S, Isolation and quantitative analysis of betulinic acid and aliphatic acid from *Zyziphi fructus*, *Yakhak Hoechi*, vol. 40, 1996, 558-562.
- 88) Bringmann G, Saeb W, Assi L. A, Francois G, Sankara Narayanan A. S, Peters K, Peters E. M, Betulinic acid: isolation from *Triphyophyllum peltatum* and

- Ancistrocladus heyneanus*, antimalarial activity, and crystal structure of the benzyl ester, *Planta medica*, vol. 63, 1997, 255-257.
- 89) Jang H, Lee J. W, Jin Q, Kim S-Y, Lee D, Hong J. T, Kim Y, Lee M. K, Hwang B Y, Biflavones and furanone glucosides from *Zabelia tyaihyonii*, *Helvetica Chimica Acta*, vol. 98, 2015, 1419-1425.
- 90) Krauze-Baranowska M, Cisowski W, Wiwart M, Madziar B, Antifungal biflavones from *Cupressocyparis leylandii*, *Planta medica*, vol. 65, 1999, 572-573.
- 91) Mpalantinos M. A, De Moura R. S, Parente J. P, Kuster R. M, Biologically active flavonoids and kava pyrones from the aqueous extract of *Alpinia zerumbet*, *Phytotherapy Research*, vol. 12, 1998, 442-444.
- 92) Gangoue-Pieboji J, Pegnyemb D. E, Niyitegeka D, Nsangou A, Eze N, Minyem C, Ngo Mbing J, Ngassam P, Ghogoum Tih R, Sodengam B. L, Bodo B, The in-vitro antimicrobial activities of some medicinal plants from Cameroon, *Annals of Tropical Medicine & Parasitology*, vol. 100, 2006, 237-243.
- 93) Sani A. A, M Sule I, Ilyas M, Haruna A. K, Abdurraheem O. R, Abdulkareem S. S, Antimicrobial Studies of Aqueous Extract of the Leaves of *Lophira lanceolata*, *Research Journal of Pharmaceutical, Biological and Chemical Sciences*, vol. 2, 2001, 637-643.
- 94) Shai L. J, McGaw L. J, Aderogba M. A, Mdee L. K, Eloff J. N, Four pentacyclic triterpenoids with antifungal and antibacterial activity from *Curtisia Dentata* (Burm.f) C.A. Sm. Leaves, *Journal of Ethnopharmacology*, vol. 119, 2008, 238-244.
- 95) Kanwal Q, Hussain I, Siddiqui H. L, Javaid A, Antimicrobial activity screening of isolated flavonoids from *Azadirachta indica* leaves, *Journal of the Serbian Chemical Society*, vol. 76, 2011, 375-384.
- 96) Tajuddeen N, Sallau M. S, Musa A. M, Yahaya S. M, Habila J. D, Musa Ismail A, A novel antimicrobial flavonoid from the stem bark of *Commiphora pedunculata* (Kotschy & Peyr.) Engl, *Natural Product Research*, 2015, 1-7.
- 97) Krauze-Baranowska M, Cisowski W, Wiwart M, Madziar B, Antifungal biflavones from *Cupressocyparis leylandii*, *Planta Medica*, vol. 65, 1999, 572-573.
- 98) Gottlieb H. E, Kotlyar V, Nudelman A, Nmr chemical shifts of common laboratory solvents as trace impurities, *The Journal of organic chemistry*, vol. 62, 1997, 7512-7515.

- 99) Sarker S. D, Latif Z, Gray A. I, Natural Products Isolation (Methods in Biotechnology), second edition, Springer Science+Business Media LLC, Totowa, N.J, 2006.
- 100) Makhafola, T. J, Samuel B. B, Elgorashi E. E, Eloff J. N, Ochnaflavone and ochnaflavone 7-O-methyl ether, two antibacterial biflavonoids from *Ochna pretoriensis* (Ochnaceae), Natural products Communications, vol. 7, 2012, 1601-1604.
- 101) Reddy B. A. K., Reddy N. P, Gunasekar D, Blond A, Bodo B, Biflavonoids from *Ochna lanceolata*, Phytochemistry Letters, vol.1, 2008, 27-30.
- 102) Reutrakul V, Ningnuek N, Pohmakotr M, Yoosook C, Napaswad C, Kasisit J, Santisuk T, Tuchinda P, Anti HIV-1 flavonoid glycosides from *Ochna integerrima*, Planta Medica, vol. 73, 2007, 683-688.
- 103) Jayakrishna G, Reddy M. K, Jayaprakasam B, Gunasekar D, Blond A, Bodo B, A new biflavonoid from *Ochna beddomei*, Journal of Asian Natural Products Research, vol. 5, 2003, 83-87.
- 104) Rao K. V, Sreeramulu K, Rao C. V, Gunasekar D, Martin M. T, Bodo B, Two new biflavonoids from *Ochna Obtusata*, Journal of Natural Products, vol. 60, 1997, 632-634.
- 105) Kamil M, Khan N. A, Alam M. S, Ilyas M, A biflavone from *Ochna pumila*, Phytochemistry, vol. 26, 1987, 1171-1173.
- 106) Okigawa M, Kawano N, Agil M, Rahman W, Structure of ochnaflavone, new type of biflavone and the synthesis of its pentamethyl ether, Tetrahedron Letters, vol. 22, 1973, 2003-2006.
- 107) Benedek B, Weniger B, Parejo I, Bastida J, Arango G. J, Lobstein A, Codina C, Antioxidant activity of isoflavones and biflavones isolated from *Godoya antioquiensis*, Arzneimittel Forschung, vol. 56, 2006, 661-664.
- 108) Lobstein A, Weniger B, Um B. H, Vonthron C, Alzate F, Anton R, Polyphenols from *Cespedesia spathulata* and *Cespedesia macrophylla*, Biochemical Systematics and Ecology, vol. 32, 2004, 229-231.
- 109) Ma J, Li N, Li X, Chemical constituents from the leaves of *Lonicera japonica* Thunb, Shenyang Yaoke Daxue Xuebao, vol. 26, 2009, 868-870, 895.
- 110) Ariyasena J, Baek S-H, Perry N. B, Weavers R. T, Ether-Linked Biflavonoids from *Quintinia acutifolia*, Journal of Natural Products, vol. 67, 2004, 693-696.

- 111) Xu J. C, Liu X. Q, Chen K. L, A new biflavonoid from *Selaginella labordei* Hieron. ex Christ, Chinese Chemical Letters, vol. 20, 2009, 939-941.
- 112) Kamara B. I, Manong D. T. L, Brandt E. V, Isolation and synthesis of a dimeric dihydrochalcone from *Agapanthus africanus*, Phytochemistry, vol. 66, 2005, 1126-1132.
- 113) Murakami A, Ohigashi H, Jisaka M, Hirota M, Irie R, Koshimizu K, Inhibitory effects of new types of biflavonoid-related polyphenols; lophirone A and lophiraic acid, on some tumor promoter-induced biological responses in vitro and in vivo, Cancer Letters, vol. 58, 1991, 101-106.
- 114) Wach A, Graber P, The plasma membrane H⁺-ATPase from yeast. Effects of pH, vanadate and erythrosine B on ATP hydrolysis and ATP binding, European Journal of Biochemistry, vol. 201, 1991, 91-97.
- 115) Billack B. C, Billack A. M, Process for the treatment and prevention of diseases caused by fungi, United States Patent No. 8,426,452 B2, Issued: 23.04.2013.
- 116) Weidenbömer M, Jha H. C, Antifungal spectrum of flavone and flavanone tested against 34 different fungi, Mycological Research, vol. 101, 1997, 733-736.
- 117) Mizobuchi S, Sato Y, A new flavanone with antifungal activity isolated from Hops, Agricultural and Biological Chemistry, vol. 48, 1984, 2771-2775.
- 118) Bernini R, Pasqualetti M, Provenzano G, Tempesta S, Ecofriendly synthesis of halogenated flavonoids and evaluation of their antifungal activity, New Journal of Chemistry, vol. 39, 2015, 2980-2987.
- 119) Greco S.S, Dorigueto A. C, Landre I. M, Soares M. G, Martho K, Lima R, Pascon R. C, Vallim M. A, Capello T. M, Romoff P, Sartorelli P, Lago J. H. G, Structural Crystalline Characterization of Sakuranetin – An Antimicrobial Flavanone from Twigs of *Baccharis retusa* (Asteraceae), Molecules, vol. 19, 2014, 7528-7542.
- 120) Bernini R, Mincione E, Provenzano G, Fabrizi G, Tempesta S, Pasqualetti M, Obtaining new flavanones exhibiting antifungal activities by methyltrioxorhenium-catalyzed epoxidation-methanolysis of flavones, Tetrahedron, vol. 64, 2008, 7561-7566.
- 121) Albogami A. S, Alkhathlan H. Z, Salehl T, S, Elazzazy A. M, Microwave-Assisted Synthesis of Potent Antimicrobial Agents of Flavanone Derivatives, Oriental Journal of Chemistry, vol. 30, 2014, 435-443.

- 122) Emami S, Shojapour S, Faramarzi M. A, Samadi N, Irannejad H, Synthesis, *in vitro* antifungal activity and *in silico* study of 3-(1,2,4-triazol-1-yl)flavanones, *European Journal of Medicinal Chemistry*, vol. 66, 2013, 480-488.
- 123) Emami S, Behdad M, Foroumadi A, Falahati M, Lotfali E, Sharifynia S, Design of Conformationally Constrained Azole Antifungals: Efficient Synthesis and Antifungal Activity of *trans*-3-Imidazolylflavanones, *Chemical Biology & Drug Design*, vol. 73, 2009, 388-395.
- 124) Peralta M. A, Calise M, Fornari M. C, Ortega M. G, Diez R. A, Cabrera J. L, Perez C, A prenylated flavanone from *Dalea elegans* inhibits 6 G efflux and reverses fluconazole-resistance in *Candida albicans*, *Planta Medica*, vol. 78, 2012, 981-987.
- 125) Rozmer Z, Perjési P, Naturally occurring chalcones and their biological activities, *Phytochemistry Reviews*, vol. 15, 2016, 87-120.
- 126) Awouafack M. D, Kusari S, Lamshöft M, Ngamga D, Tane P, Spiteller M, Semi-Synthesis of Dihydrochalcone Derivatives and Their *in Vitro* Antimicrobial Activities, *Planta Medica*, vol. 76, 2010, 640-643.